

1 Using  $^{14}\text{C}$  and  $^3\text{H}$  to understand groundwater flow and recharge in an  
2 aquifer window

3

4 **A.P. Atkinson<sup>1,2</sup>, I. Cartwright<sup>1,2</sup>, B.S. Gilfedder<sup>3</sup>, D. I. Cendón<sup>4,5</sup>, N. P. Unland<sup>1,2</sup>,**  
5 **H. Hofmann<sup>6</sup>**

6 <sup>1</sup>School of Geosciences, Monash University, Clayton, Vic, 3800, Australia.

7 <sup>2</sup>National Centre for Groundwater Research and Training, GPO Box 2100, Flinders University, Adelaide, SA  
8 5001, Australia.

9 <sup>3</sup>Department of Hydrology, University of Bayreuth, Bayreuth, Germany.

10 <sup>4</sup>Australian Nuclear Science and Technology Organisation, Menai, NSW 2232, Australia.

11 <sup>5</sup>School of Biological Earth and Environmental Sciences, The University of New South Wales, Sydney, NSW  
12 2052, Australia.

13 <sup>6</sup>School of Earth Sciences, The University of Queensland, Brisbane, QLD 4072, Australia.

14

15

16

17

18

19

20

21

22

23 Correspondence to: A.P. Atkinson ([alexander.atkinson@monash.edu](mailto:alexander.atkinson@monash.edu))

24

25

26

27

28

29

30

31

## 32 **Abstract**

33 Knowledge of groundwater residence times and recharge locations are vital to the sustainable  
34 management of groundwater resources. Here we investigate groundwater residence times and patterns  
35 of recharge in the Gellibrand Valley, southeast Australia, where outcropping aquifer sediments of the  
36 Eastern View Formation form an ‘aquifer window’ that may receive diffuse recharge from rainfall  
37 and recharge from the Gellibrand River. To determine recharge patterns and groundwater flowpaths,  
38 environmental isotopes ( $^3\text{H}$ ,  $^{14}\text{C}$ ,  $\delta^{13}\text{C}$ ,  $\delta^{18}\text{O}$ ,  $\delta^2\text{H}$ ) are used in conjunction with groundwater  
39 geochemistry and continuous monitoring of groundwater elevation and electrical conductivity. The  
40 water table fluctuates by 0.9 to 3.7 m annually, implying recharge rates of 90 and 372 mm yr<sup>-1</sup>.  
41 However, residence times of shallow (11 to 29 m) groundwater determined by  $^{14}\text{C}$  are between 100  
42 and 10,000 years,  $^3\text{H}$  activities are negligible in most of the groundwater, and groundwater electrical  
43 conductivity remains constant over the period of study. Deeper groundwater with older  $^{14}\text{C}$  ages has  
44 lower  $\delta^{18}\text{O}$  values than younger shallower groundwater, which is consistent with it being derived from  
45 greater altitudes. The combined geochemistry data indicate that local recharge from precipitation  
46 within the valley occurs through the aquifer window, however much of the groundwater in the  
47 Gellibrand Valley predominantly originates from the regional recharge zone, the Barongarook High.  
48 The Gellibrand Valley is a regional discharge zone with upward head gradients that limits local  
49 recharge to the upper 10 m of the aquifer. Additionally, the groundwater head gradients adjacent to  
50 the Gellibrand River are generally upwards, implying that it does not recharge the surrounding  
51 groundwater and has limited bank storage.  $^{14}\text{C}$  ages and Cl concentrations are well correlated and Cl  
52 concentrations may be used to provide a first-order estimate of groundwater residence times.  
53 Progressively lower chloride concentrations from 10,000 years BP to the present day are interpreted to  
54 indicate an increase in recharge rates on the Barongarook High.

55

56

## 57 **1. Introduction**

58 Groundwater residence time can be defined as the period of time elapsed since the infiltration  
59 of a given volume of water (Campana & Simpson, 1984), or perhaps more accurately, the  
60 mean time that a mixture of waters of different ages have resided in an aquifer (Bethke &  
61 Johnson, 2008). The residence time of water within an aquifer is a key parameter in  
62 describing catchment storage and may be used to estimate historical recharge rates (Le Gal  
63 La Salle et al., 2001; Cook et al., 2002; Cartwright & Morgenstern, 2012; Zhai et al., 2013),  
64 elucidate groundwater flowpaths (Gardner et al., 2011; Smerdon et al., 2012), calibrate  
65 hydraulic models (Mazor & Nativ, 1992; Reilly et al., 1994; Post et al., 2013) and  
66 characterize the rate of contaminant spreading (Böhlke and Denver 1995; Tesoriero et  
67 al.,2005). From a water resource perspective, information on groundwater residence times is  
68 required for sustainable aquifer management by identifying the risk posed to groundwater  
69 reserves against over-exploitation (Foster & Chilton, 2003), climate change (Manning et al.,  
70 2012) and contamination (Böhlke, 2002).

71

72 Unconfined aquifers may be recharged over broad regions leading to young groundwater at  
73 shallow depths over broad areas (Cendón et al., 2014). On the other hand, the residence time  
74 of groundwater in confined aquifers generally increases away from discrete recharge areas.  
75 The geology of catchments is often complex and heterogeneous and outcrops of aquifers in  
76 more than one location may provide ‘windows’ for groundwater recharge (Meredith et al.,  
77 2012). It is important to document groundwater flow from such aquifer windows. If they act  
78 as recharge areas, changes in land-use such as agricultural development may introduce  
79 contaminants to the deeper regional groundwater systems. By contrast, if they are local

80 discharge areas, use of regional groundwater from these areas may impact rivers, lake or  
81 wetlands that are receiving groundwater.

82

83 Rivers may also recharge shallow groundwater if the hydraulic gradient between the river and  
84 the groundwater is reversed during high flows (Doble et al., 2012). Episodic recharge of  
85 aquifers by large over-bank floods is also locally important (Moench & Barlow, 2000;  
86 Cendón et al., 2010; Doble et al., 2012), particularly in arid areas (Shentsis & Rosenthal,  
87 2003); however, the potential for over-bank events to recharge aquifers in temperate areas is  
88 still poorly understood. Additionally, during high flow, water from rivers is likely stored  
89 temporarily in the banks (McCallum et al., 2010, Unland et al., 2014); however, the depth  
90 and lateral extent to which bank exchange water infiltrates the aquifer is not well documented.  
91 Lastly, knowledge of residence times of groundwater in close proximity to the river can  
92 provide important information on groundwater-river interactions (Gardner et al., 2011). Local  
93 groundwater flowpaths in connection with rivers are often underlain by deeper regional  
94 flowpaths (Tóth, 1963) however the role these flowpaths play in contributing to river baseflow  
95 remains unclear (Sklash & Farvolden, 1979; McDonnell, 2010; Frisbee & Wilson, 2013;  
96 Goderniaux et al., 2013). This may be elucidated from understanding residence times of near-  
97 river groundwater (Smerdon et al., 2012).

98

99 Radioactive environmental isotopes, in particular  $^{14}\text{C}$  and  $^3\text{H}$  have proven useful tools for  
100 determining groundwater residence times (Vogel, 1974; Wigley, 1975). Produced in the  
101 atmosphere via the interaction of  $\text{N}_2$  with cosmic rays,  $^{14}\text{C}$  has a half life of 5730 years and  
102 can be used to trace groundwater with residence times up to 30 ka. The use of  $^{14}\text{C}$  in dating  
103 groundwater was first discussed by Muennich (1957), and has subsequently been widely used

104 due to the ubiquitous presence of dissolved inorganic carbon (DIC) in groundwater  
105 (Cartwright et al., 2012; Samborska et al., 2012; Stewart, 2012). The calculation of  $^{14}\text{C}$  ages  
106 may be complicated if groundwater DIC is derived from a mixture of sources (Clark and Fritz,  
107 1997). Where a large proportion of DIC is derived from the dissolution of  $^{14}\text{C}$ -free carbonate  
108 minerals in the aquifer matrix, the  $^{14}\text{C}$  originating from the atmosphere or soil zone will be  
109 significantly diluted. Additional sources of  $^{14}\text{C}$  free DIC include old geogenic carbon from  
110 igneous degassing (Bertrand et al., 2013; Frederico et al., 2002) or  $\text{CO}_2$  produced together  
111 with methane from old organic carbon in the aquifer matrix (Aravena et al., 1995).  
112 Groundwaters recharged post 1950 may have anomalously high  $^{14}\text{C}$  activities ( $a^{14}\text{C}$ ) due to  
113 the  $^{14}\text{C}$  produced during atmospheric nuclear tests. Objective  $^{14}\text{C}$  dating requires recognition  
114 and quantification of these processes. A number of models based on both major ion and  
115 stable C isotope geochemistry have been proposed to correct apparent  $^{14}\text{C}$  ages (Han &  
116 Plummer, 2013)

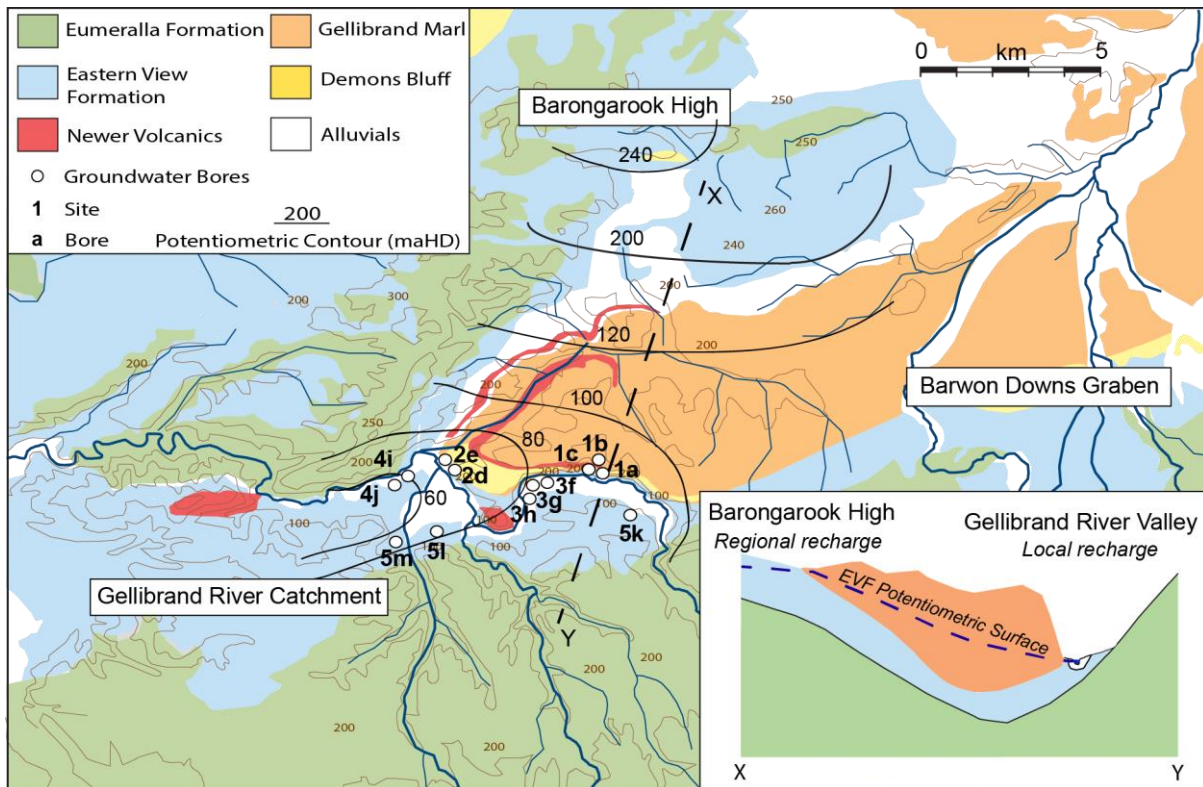
117

118 With a significantly shorter half-life (12.33 years),  $^3\text{H}$  can be used to date groundwater with  
119 residence times of up to 100 years (Vogel et al., 1974). With the decay of the 1960s  $^3\text{H}$  bomb-  
120 pulse peak in the southern hemisphere to near background levels unique ages may now be  
121 determined from single  $^3\text{H}$  measurements (Morgenstern et al., 2010). As  $^3\text{H}$  is part of the  
122 water molecule, there is negligible change to  $^3\text{H}$  activities other than decay, and  $^3\text{H}$  is an  
123 excellent tracer for the movement of water through hydrological systems (Michel, 2004).  
124 Used in conjunction with  $^{14}\text{C}$  data,  $^3\text{H}$  may also be used to study mixing in shallow aquifers  
125 (Le Gal La Salle 2001; Cartwright & Morgenstern, 2012).

126

127

128 **2. Study Site**



129  
 130 **Figure 1** – Geology, groundwater flow, and cross sectional view of the upper part of the Gellibrand  
 131 River Catchment (the Gellibrand Valley). Potentiometric contours for the Eastern View Formation are  
 132 created from groundwater data (Water Resources Data Warehouse, 2013) and are expressed in metres  
 133 above Australian Height Datum (mAHD). Sampled groundwater bores are also shown. Letters refer to  
 134 bores in Table 1.

135

136

137 The Otway Basin is located in southwest Victoria, covering an area of 150,000 km<sup>2</sup>. The  
 138 basin was formed during the Cretaceous rifting of Australia and Antarctica (Briguglio et al.,  
 139 2013) and is infilled with Upper Cretaceous and Cenozoic siliciclastic and calcareous  
 140 sediments that form several aquifers and aquitards. The basin is divided into a number of sub-  
 141 basins with regional groundwater flow paths originating at topographic highs. The Gellibrand  
 142 River Catchment is one of these sub-basins. This study focuses on a 250 km<sup>2</sup> upland area of

143 the Gellibrand River Catchment (known as the Gellibrand Valley), which lies at the foothills  
144 of the Otway Ranges, directly south of the Barongarook High (Fig.1).

145

146 Cretaceous Otway Group sediments of the Eumeralla Formation form the basement of the  
147 catchment and crop out in areas of higher relief. The Eumeralla Formation consists of thickly  
148 bedded siltstone, mudstone and volcanolithic sandstone. It has a low primary porosity and  
149 hydraulic conductivity and acts as a poor aquifer (Lakey & Leonard, 1982). Cenozoic  
150 sediments of the Wangerrip group overlie the bedrock and form major aquifers in the region  
151 to which flow is constrained (Van den Berg, 2009). The primary aquifer in the study area is  
152 the Eastern View Formation or the equivalent Dilwyn Formation (Van den Berg 2009;  
153 Petrides & Cartwright 2006; Atkinson et al., 2013) that is composed of gravel, fine to coarse  
154 grained sand, and major clay layers. The Eastern View Formation comprises predominantly  
155 quartz, feldspars and carbonates (< 2 %) and has hydraulic conductivities of  $10^{-2}$  to  $10^2$  m d<sup>-1</sup>  
156 (Hortle et al., 2011). The Eastern View Formation is underlain by another productive aquifer,  
157 the Pebble Point Formation, however this is much thinner and is separated from the above  
158 layers by the Pember Mudstone. To the north, the Eastern View Formation is confined by the  
159 Gellibrand Marl, which is a regional aquitard that comprises 100 to 200 m of clay, and the  
160 Demons Bluff formation, which comprises fine-grained silts. Basaltic intrusions of the  
161 Quaternary Newer Volcanics are also present. The floodplain is covered with recent alluvial  
162 deposits of sand and clay. Regional groundwater recharge occurs on the Barongarook High  
163 where the Eastern View Formation crops out. Groundwater flows southwest along the  
164 Gellibrand River Catchment from the Barongarook High as well as eastward into the Barwon  
165 Downs Graben. However there is also potential for localised recharge within the Gellibrand  
166 Valley, where outcropping sediments of the Eastern View Formation, potentially act as an  
167 aquifer window (Fig. 1).

168 The Gellibrand Valley contains a mixture of cool temperate rainforest on the valley sides and  
169 cleared agricultural pasture through which the Gellibrand River flows. Rainfall across the  
170 catchment averages  $\sim 1000 \text{ mm yr}^{-1}$ , with the majority of rainfall falling in the Australian  
171 winter between June and September (Bureau of Meteorology, 2013). The Gellibrand River is  
172 gaining and groundwater contributes between 10 and 50% to total river flow dependent on  
173 flow conditions (Atkinson et al., 2013). River flows are between  $5 \times 10^4 \text{ m}^3 \text{ day}^{-1}$  and  $2 \times 10^6$   
174  $\text{m}^3 \text{ day}^{-1}$  (Fig. 2c), with low flows during summer months (December to March) and high  
175 flows and flooding during winter (June to August) (Victorian Water Resources Data  
176 Warehouse, 2013). During flooding there is the potential for aquifer recharge from overbank  
177 flow.

178

179 Although groundwater residence times in the Otway Basin have been explored in the  
180 Gambier Embayment (Love et al., 1994) and nearby Barwon River Graben (Petrides &  
181 Cartwright, 2006), little is known of the residence times of groundwater in the Gellibrand  
182 River Catchment. This is despite the groundwater in Eastern View Formation being a  
183 potential valuable water resource (Petrides & Cartwright, 2006). Here we evaluate  
184 groundwater residence times in the Gellibrand Valley where the Eastern View Formation is  
185 exposed, forming an aquifer window, and regular episodic river floods occur, to understand  
186 the origins of groundwater within the valley and to identify whether groundwater recharge  
187 via rainfall and/or the river occurs in this part of the groundwater system. This is important in  
188 understanding the potential impacts of landuse change and pollution in the catchment as well  
189 as understanding the dynamics of recharge in catchments where aquifer material is exposed  
190 in more than one location. It is also important to fully understand groundwater systems such  
191 as this that have the potential to be developed as significant water resources. Radioactive  
192 tracers  $^{14}\text{C}$  and  $^3\text{H}$  are used to determine residence times and define groundwater flow paths



193 whilst major ion chemistry is employed to determine dominant geochemical processes. Water  
194 table fluctuations and groundwater electrical conductivities are also continuously monitored.  
195 These easily measurable, robust parameters can be used to observe changes in storage and  
196 infer sources of aquifer recharge (Vogt et al., 2010) and allow for comparison with  
197 radioisotopes in understanding the dynamics of groundwater systems. Together, isotopic and  
198 physico-chemical approaches provide insight on both short-term recharge processes (electrical  
199 conductivity, water levels) and long-term recharge processes ( $^3\text{H}$  and  $^{14}\text{C}$ ).

200

### 201 **3. Methods**

202 A number of groundwater monitoring bores that form part of the Victorian State Observation  
203 Bore network are present in the Gellibrand Valley (Victorian Water Resources Data  
204 Warehouse, 2013). These are screened in the Eastern View Formation, with depths of  
205 between 0 and 42 m. Bores located within 25 m from the Gellibrand River generally have  
206 screen depths between 11 and 15 m, whilst bores located on the flood plain have depths  
207 between 21 and 42 m. Groundwater from the Eastern View Formation was sampled from 13  
208 bores. 10 of these are located within 25 m from the river in a  $14 \text{ km}^2$  area of the catchment  
209 (Sites 1 to 4 in Fig. 1), with 3 further samples taken from bores situated further back on the  
210 flood plain between 1 and 2 km from the river (Site 5 in Fig. 1). Groundwater was sampled  
211 using an impeller pump set in the screen, with 2 to 3 bore volumes purged before sampling.  
212 In the field, samples for anion analysis were filtered through  $0.45\mu\text{m}$  cellulose nitrate filters,  
213 whilst samples for cation analysis were filtered and acidified with high purity 16 N  $\text{HNO}_3$  to  
214  $\text{pH} < 2$ . Additionally, electrical conductivity (EC) and pH of groundwater were measured in  
215 the field using a calibrated TPS WP-81 conductivity/pH meter and probes. To assess transient  
216 changes in groundwater levels and EC, Aqua Troll 200 (In-Situ) data loggers were deployed

217 in June 2011. A significant drop in EC in near-river groundwater is shown in some bores  
218 following flooding in June 2012 when bores were overtopped. However immediately upon  
219 pumping in October 2012 (bores 3g, 4i) and April 2013 (bore 1b), the EC of the groundwater  
220 returned to pre-flood EC values. We interpret this as floodwater that infiltrated down the bore  
221 which was not displaced by groundwater prior to pumping, and these data have been omitted.  
222 Rainfall samples were also collected in the catchment throughout the study period for  
223 chemical analysis.

224

225 Cations were analysed on filtered, acidified samples using a Thermo Finnigan X Series II  
226 Quadrupole ICP-MS. Anions were measured on filtered unacidified samples using a  
227 Metrohm ion chromatograph. The precision of major ion concentrations based on replicate  
228 analyses is  $\pm 2$  %. Charge balances are within  $\pm 5$  %. Stable isotope ratios were measured  
229 using Finnigan MAT 252 and ThermoFinnigan DeltaPlus Advantage mass spectrometers.  
230  $\delta^{18}\text{O}$  values were measured via equilibration with He-CO<sub>2</sub> at 32°C for 24 to 48hr in a  
231 Finnigan MAT Gas Bench whilst  $\delta^2\text{H}$  values were measured by the reaction of water samples  
232 with Cr at 850°C using a Finnigan MAT H/Device. Both  $\delta^{18}\text{O}$  and  $\delta^2\text{H}$  were measured against  
233 an internal standard that has been calibrated using the IAEA, SMOW, GISP and SLAP  
234 standards. Data was normalised following methods outlined by Coplen (1988) and are  
235 expressed relative to V-SMOW where  $\delta^{18}\text{O}$  and  $\delta^2\text{H}$  values of SLAP are -55.5‰ and -428‰  
236 respectively. Precision is  $\pm 1$ ‰ for  $\delta^2\text{H}$  and  $\pm 0.2$ ‰ for  $\delta^{18}\text{O}$ .

237

238  $^{14}\text{C}$  and  $^3\text{H}$  samples of groundwater were measured at the Australian Nuclear Science and  
239 Technology Organisation (ANSTO) and the Tritium and Water Dating Laboratory, Institute  
240 of Geological and Nuclear Sciences (GNS), (New Zealand). For  $^{14}\text{C}$  analysis performed at

241 ANSTO, CO<sub>2</sub> was extracted from water samples in a vacuum line using orthophosphoric acid  
242 and converted to graphite through reduction with excess H<sub>2</sub> gas in the presence of an iron  
243 catalyst at 600°C. <sup>14</sup>C concentrations were measured using a 10kV tandem accelerator mass  
244 spectrometer. δ<sup>13</sup>C values for these samples are derived from the graphite fraction used for  
245 radiocarbon via EA-IRMS.

246

247 For <sup>14</sup>C samples measured at GNS, CO<sub>2</sub> was extracted from groundwater samples through  
248 addition of orthophosphoric acid. CO<sub>2</sub> was made into a graphite target and analysed by AMS.  
249 An aliquot of the extracted CO<sub>2</sub> was used for δ<sup>13</sup>C analysis. <sup>14</sup>C activities are expressed as  
250 pMC (percent modern carbon) where pMC = 100% corresponds to 95% of the <sup>14</sup>C  
251 concentration of NBS oxalic acid standard (Stuiver and Polach, 1977), with a precision of  
252 <sup>14</sup>C/<sup>12</sup>C ratios of ±0.5 (Fink et al 2004). At both ANSTO and GNS, samples for <sup>3</sup>H were  
253 distilled and electrolytically enriched prior to being analysed by liquid scintillation counting  
254 as described by Neklapilova et al. (2008a,b) and Morgenstern and Taylor (2009). <sup>3</sup>H activities  
255 are expressed in Tritium Units (TU) with a relative uncertainty of ± 5 % and a quantification  
256 limit of 0.13 to 0.14 TU at ANSTO and 0.02 TU and a relative uncertainty of 2 % at GNS.

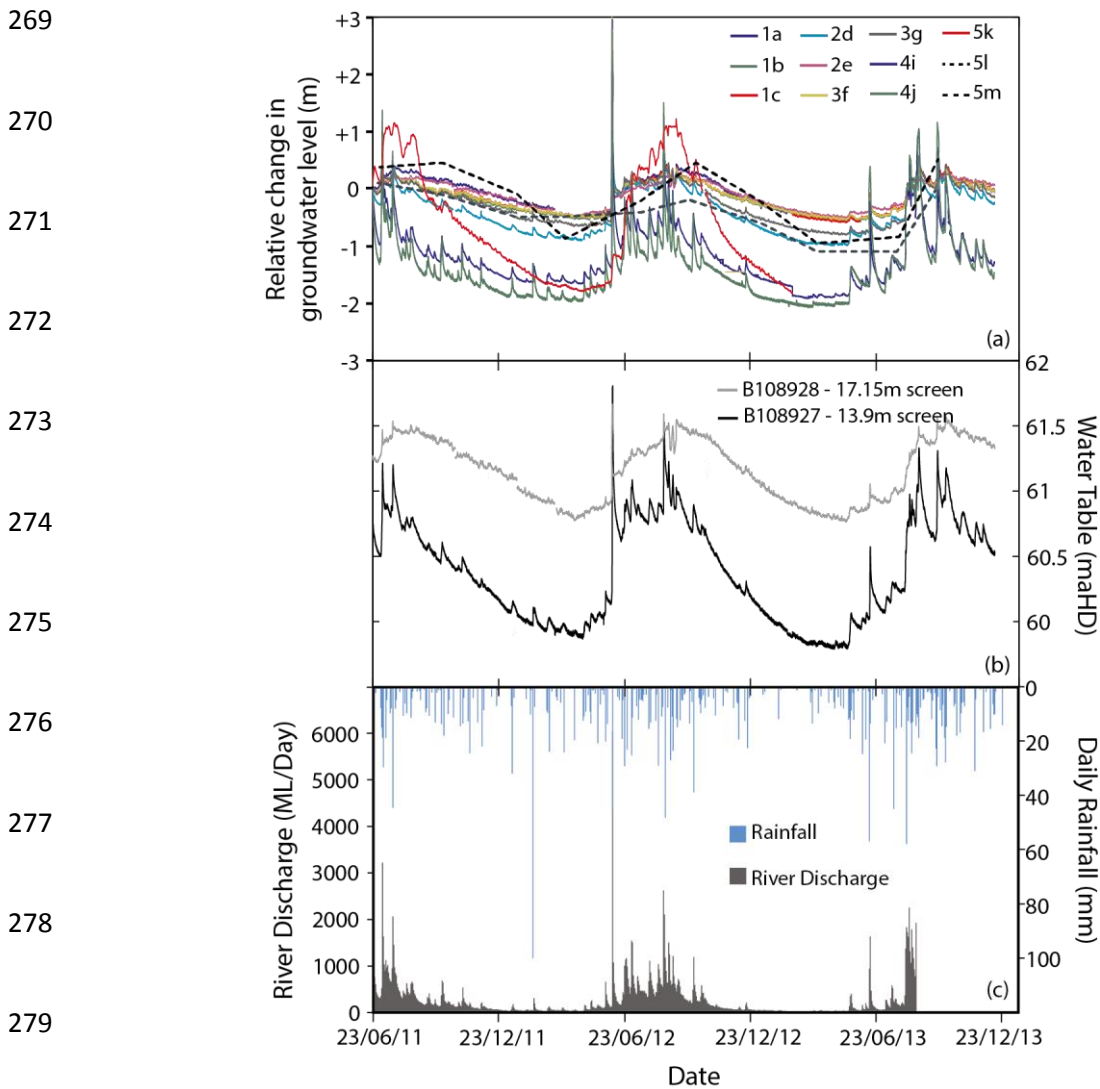
257

## 258 **(4) Results**

### 259 *(4.1) Groundwater elevations*

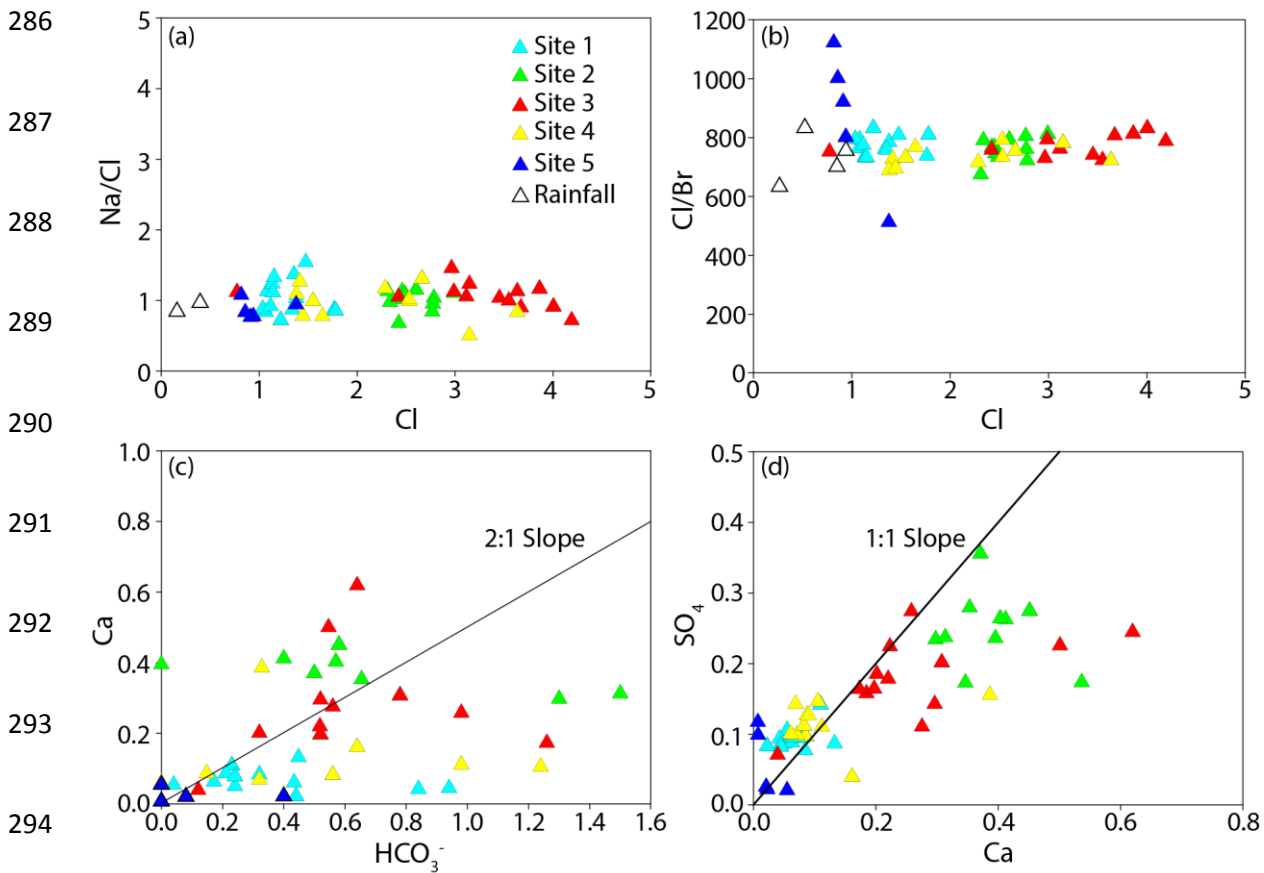
260 Groundwater elevations decrease from 230 m relative to the Australian Height Datum (AHD)  
261 on the Barongarook High to <60 mAHD within the Gellibrand Valley (Fig.1), with  
262 groundwater flowing from the Barongarook High towards the Gellibrand Valley and then  
263 westward. Groundwater elevations from all depths and positions within the Gellibrand Valley

264 are in phase and fluctuate between 1 and 3 m annually (Fig. 2a). The water table rises  
 265 between June and August following winter rainfall (Fig. 2c) and head gradients at nested sites  
 266 are upwards (Fig. 2b). The Gellibrand River has high water levels that result in flooding  
 267 during winter months (June to August) and low flows in summer (December to March) (Fig.  
 268 2c).



280  
 281 **Figure 2** - (a) Groundwater elevations in bores display clear annual cycles (b) Groundwater head-  
 282 gradients in the Gellibrand Valley are upwards implying a discharge zone (Victorian Water Resources  
 283 Data Warehouse, 2013) (c) Flow in the Gellibrand River. Baseflow conditions during summer months  
 284 transition into high flows in winter following winter rainfall. (Bureau of Meteorology, 2013)

285 (4.2) Groundwater Geochemistry



295  
 296 **Figure 3** – Geochemical characteristics of groundwater in the Eastern View Formation; (a) mCl/Br v  
 297 mCl (b) mNa/Cl v mCl (c) mCa v mHCO<sub>3</sub><sup>-</sup> (d) mSO<sub>4</sub> v mCa. Rainfall samples are also plotted where  
 298 measured. Data is from Table 1 with repeat measurements over the sampling period included.

299  
 300 The chemistry of groundwater in the Gellibrand Valley is summarised in Table 1.  
 301 Groundwater is oxic, with electrical conductivities between 140 and 600  $\mu\text{S cm}^{-1}$  and pH  
 302 values ranging from 4.8 to 6.0. Groundwater from close proximity to the river (Sites 1 to 4)  
 303 generally has higher EC values (144 to 545  $\mu\text{S cm}^{-1}$ ) than groundwater further back on the  
 304 floodplain at site 5 (149 to 220  $\mu\text{S cm}^{-1}$ ). Despite the range of salinity, the relative  
 305 proportions of the major ions in groundwater are similar across the catchment. The  
 306 groundwater is Na-Cl type. Cl constitutes between 68 and 92% of total anions on a molar

307 basis, with  $\text{HCO}_3$  accounting for 0 to 25%. Increases in Cl concentrations are associated with  
308 a decrease in  $\text{HCO}_3$ . Na comprises between 60 and 85% of total cations with Ca constituting  
309 1 to 10%, Mg constituting 0 to 10% and K constituting 0 to 10%. Increased Na  
310 concentrations are associated with decreases in both Ca and Mg concentrations. Molar Cl/Br  
311 ratios are between 400 and 600 and do not increase with increasing Cl (Fig. 3b), molar Na/Cl  
312 ratios are 0.7 to 1.3 and also remain stable with increasing Cl concentrations (Fig. 3a). Na/Cl  
313 ratios of groundwater samples are similar to those measured in rainfall in southeast Australia  
314 (Blackburn and Mcleod, 1983) and the Cl/Br ratios are also similar to those expected for local  
315 rainfall (Cartwright et al., 2006). There is a weak correlation between Ca and  $\text{HCO}_3$  (Fig. 3c)  
316 and between Ca and  $\text{SO}_4$  (Fig. 3d).

317

#### 318 *(4.3) $^{13}\text{C}$ , $\delta^{14}\text{C}$ and $^3\text{H}$ concentrations*

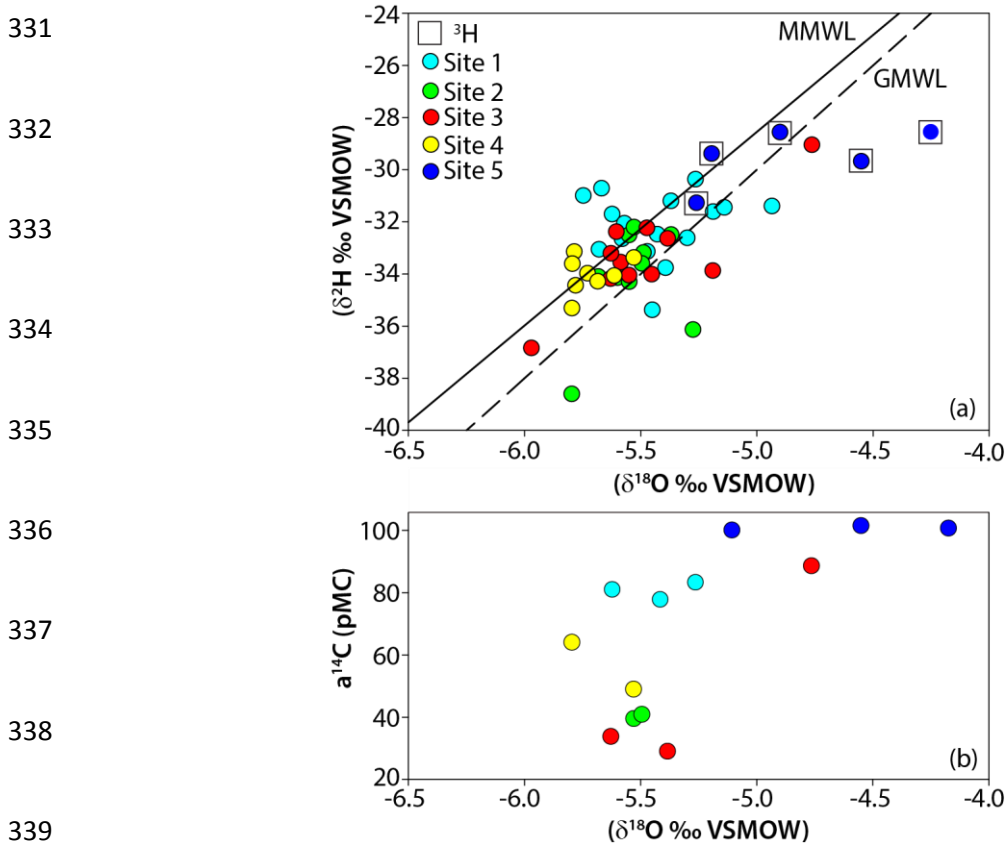
319 The  $\delta^{14}\text{C}$  of groundwater ranges from 29 to 101.5 pMC.  $^3\text{H}$  activities are below detection for  
320 the majority of groundwater samples (Table 1), with the exception of bores 5k, 5l and 5m  
321 which have activities of 1.02, 1.47 and 1.24 TU, respectively. Groundwater from these bores  
322 has  $\delta^{14}\text{C} > 90$  pMC. The distribution of  $\delta^{14}\text{C}$  and  $^3\text{H}$  values across the catchment is  
323 heterogeneous with no relationship to depth or along lateral groundwater flowpaths. A strong  
324 inverse correlation ( $R^2 = 0.87$ ) is observed between  $\delta^{14}\text{C}$  and Cl concentrations (Table 1). A  
325 similar correlation is also observed for Na ( $R^2 = 0.855$ ), K ( $R^2 = 0.82$ ), Ca ( $R^2 = 0.6$ ) and Mg  
326 ( $R^2 = 0.54$ ).

327

328

329

330 (4.4) Stable Isotopes ( $\delta^2\text{H}$ ,  $\delta^{18}\text{O}$ ,  $\delta^{13}\text{C}$ )



340 **Figure 4** – (a)  $^2\text{H}$  vs  $^{18}\text{O}$  values of the Gellibrand River and surrounding groundwater sampled over  
 341 March 2011 – August 2013 and the weighted average for rainfall from Adelaide and Melbourne.  
 342 MMWL = Melbourne Meteoric Water Line (Hughes and Crawford, 2012). GMWL = Global Meteoric  
 343 Water Line (Clarke and Fritz, 1997). Groundwaters with  $^3\text{H}$  activities  $> 1$  TU are also highlighted.  
 344 Data is from Table 1 with repeat measurements over the sampling period included. (b)  $a^{14}\text{C}$  vs  $^{18}\text{O}$  of  
 345 groundwater samples.

346

347  $\delta^{18}\text{O}$  and  $\delta^2\text{H}$  values of groundwater define a narrow field ( $\delta^{18}\text{O} = -4$  to  $-6$  ‰ and  $\delta^2\text{H} = -28$   
 348 to  $-40$  ‰) that is close to both the global and local meteoric water lines (Fig. 4a). The  
 349 Gellibrand Valley is located between Melbourne and Adelaide, with groundwater generally  
 350 plotting between the average isotopic compositions of meteoric waters located in those areas.  
 351 Groundwater samples from site 5 are enriched in both  $\delta^{18}\text{O}$  ( $+ 0.7$  ‰) and  $\delta^2\text{H}$  ( $+ 3.5$  ‰)  
 352 relative to groundwater from sites 1 to 4 and have  $^3\text{H}$  activities  $> 1$  TU (Fig. 4a). Additionally

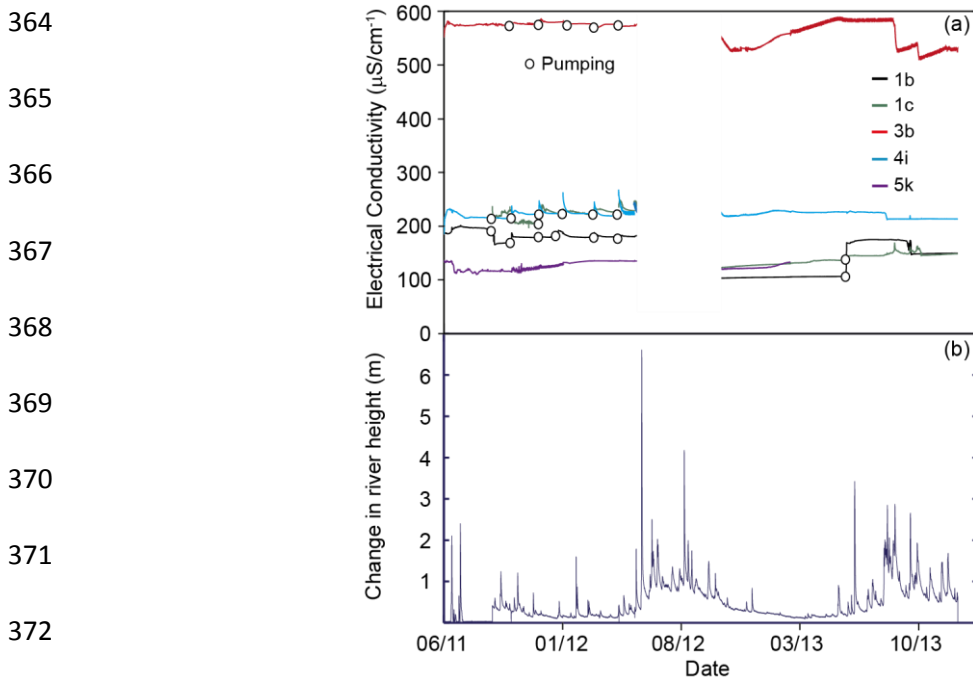
353 samples that are enriched in  $\delta^{18}\text{O}$  have a  $^{14}\text{C}$  >100 pMC (Fig. 4b).  $\delta^{13}\text{C}$  values of DIC from  
354 groundwater range from -19.8 to -25 ‰, with an average of 21.7‰ (Table 1)

355

#### 356 (4.5) Continuous Electrical Conductivity

357 Continuous groundwater EC records for a number of near-river bores and 5k, which is  
358 situated on the flood-plain, are shown in conjunction with changes in river height for the  
359 study period (Fig. 5). Groundwater EC in all bores for the majority of the dataset show little  
360 or no response to changes in river height, although minor dilution of groundwater EC occurs  
361 during high flow events in August and September 2013. Minor changes in EC correlate to  
362 sampling events in which groundwater bores were pumped

363



373

374 **Figure 5** – (a) Continuous electrical conductivity monitoring of near-river groundwater. (b). Changes  
375 in river height over the study period. Groundwater EC and river level data from deployed Aqua troll  
376 200 (In-Situ) Data Loggers.

377



378 **(5) Discussion**

379

380 *(5.1) Groundwater Chemistry*

381 Understanding geochemical processes in groundwater is required for correction of  $^{14}\text{C}$  ages  
382 and in documenting groundwater flow and recharge. Processes which govern the evolution of  
383 groundwater geochemistry and sources of solutes in the Eastern View Formation can be  
384 determined from the major ion geochemistry. The observation that Cl/Br ratios are between  
385 500 and 1000, which is similar to those expected in rainfall, and do not increase with  
386 increased TDS implies that evapotranspiration rather than halite dissolution is the major  
387 process controlling groundwater salinity (Herczeg et al., 2001; Cartwright et al., 2006). This  
388 conclusion is also consistent with an absence of halite in the aquifer lithologies. The  $\delta^{18}\text{O}$  and  
389  $\delta^2\text{H}$  values of groundwater generally lie close to the meteoric water line and do not define  
390 evaporation trends, implying that transpiration in the soil zone or upper parts of the aquifer is  
391 likely to be more dominant over evaporation. Na/Cl ratios in groundwater are also similar to  
392 those in local rainfall (~1) implying that silicate weathering is limited (e.g., Edmunds et al.,  
393 2002), whilst the increase in Na concentrations at the expense of Ca may indicate ion  
394 exchange reactions on the surface of clay minerals (e.g., Herczeg et al., 2001). That Ca and  
395  $\text{mHCO}_3$  are poorly correlated suggests that negligible dissolution of calcite has occurred. A  
396 handful of groundwater samples have a 1:1 Ca: $\text{SO}_4$  ratio indicating some minor gypsum  
397 dissolution may take place. Together, the major ion geochemistry suggests that water-rock  
398 interaction is limited with minimal silicate weathering, negligible dissolution of halite and  
399 carbonate minerals and some minor dissolution of gypsum. As is the case elsewhere in  
400 southeast Australia, including within the Otway basin, the primary geochemical process is  
401 evapotranspiration promoted by the moderate rainfall and water-efficient native vegetation,

402 and the groundwater salinity is largely controlled by the degree of evapotranspiration during  
403 recharge (Herczeg et al., 2001; Bennetts et al., 2006; Petrides & Cartwright, 2006).

404

405 Groundwater from the near-river sites 1 to 4 has lower  $\delta^{18}\text{O}$  and  $\delta^2\text{H}$  values relative to that  
406 from the floodplain away from the river at site 5. In a catchment of  $< 250 \text{ km}^2$  with a  $^{14}\text{C}$   
407 varying between 29.1 to 101.5 pMC, climatic influences and the altitude effect are the most  
408 likely drivers in variability between groundwater samples (e.g., Dansgaard, 1964). As there is  
409 potential for groundwater recharge on the elevated Barongarook High and within the  
410 Gellibrand Valley; the depleted stable isotope signature of groundwater at sites 1 to 4 relative  
411 to groundwater samples from site 5 may reflect altitudinal differences of groundwater  
412 recharged at these locations. Assuming typical altitudinal gradients in rainfall of  $-0.15\text{‰}$  to -  
413  $0.5\text{‰}$  per 100 m for  $\delta^{18}\text{O}$  (Clark & Fritz, 1997) and an elevation difference of  $\sim 150\text{m}$   
414 between the Gellibrand Valley and the Barongarook High, groundwater recharged on the  
415 Barongarook High is expected to be depleted in  $^{18}\text{O}$  by  $-0.25\text{‰}$  to  $-0.75\text{‰}$  relative to that  
416 which is locally recharged in the valley.  $\delta^{18}\text{O}$  values of groundwater from sites 1 to 4 are  
417  $\sim -0.7\text{‰}$  lower than groundwater from site 5. Thus, the stable isotopes indicate that water in  
418 the near-river environment may have been recharged from the Barongarook High, whilst  
419 water from the floodplain is recharged locally within the valley. This is supported by the  
420 negligible  $^3\text{H}$  activities at sites 1 to 4, which indicate old water, and elevated activities at site  
421 5 indicating recently recharged water. It is possible that the differences in stable isotopes  
422 between the sites are driven by climatic factors rather than altitude.

423

424 It is also possible that the variations in  $\delta^{18}\text{O}$  values represent variation in the climate during  
425 recharge. While this has been proposed elsewhere in the Otway Basin (Love et al., 1994), in

426 this part of the Otway Basin climatic variation has not been recorded in groundwater  $\delta^{18}\text{O}$   
427 values (Petrides and Cartwright, 2006). The lack of a systematic variation in  $\delta^{18}\text{O}$  values with  
428  $\text{a}^{14}\text{C}$  in groundwater from sites 1 to 4 also indicates that a climatic influence on  $\delta^{18}\text{O}$  values is  
429 unlikely.

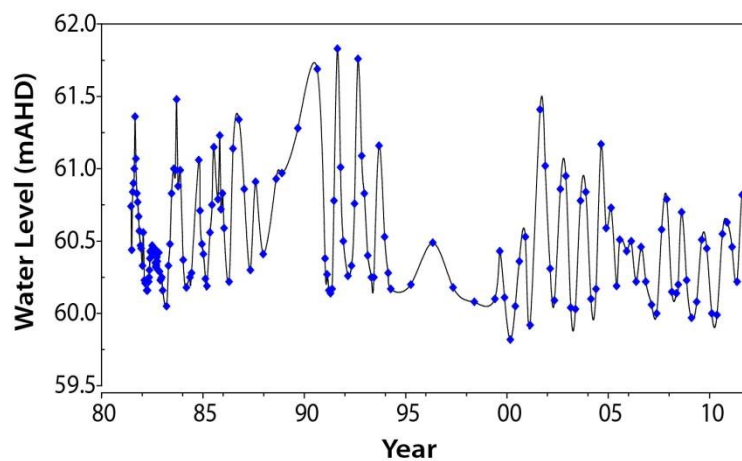
430

### 431 (5.2) Water Table Fluctuations

432 Annual cycles of groundwater elevations are present in all groundwater bores, which are  
433 screened 11 to 40 m below the ground surface. The fluctuations in groundwater levels across  
434 the Gellibrand Valley are likely a pressure response to recharge on the flood plain following  
435 rainfall events via hydraulic loading (Cartwright et al., 2007; Brodie et al., 2008; Unland et  
436 al., 2014). The magnitude of annual water table fluctuations recorded in data loggers is  
437 similar to those over the previous 30 years (Fig.6).

438

439



443

444 **Figure 6** – Historical water table fluctuations 1988-2011 for bore 108927 (Victorian Water Resources  
445 Data Warehouse, 2013). The magnitude of annual recharge cycles are coherent with those recorded in  
446 data loggers over the study period (2011 to 2013)

447

448

449 Recharge was estimated for years 2012 and 2013 using the water-table fluctuation method  
450 Eq.(1):

$$451 \quad R = S_y * \Delta h / \Delta t \quad (1)$$

452 (Scanlon et al., 2002), where  $S_y$  is specific yield,  $\Delta h$  is the change in water table height  
453 between the hydrograph recession and hydrograph peak and  $\Delta t$  is time. The water table rise is  
454 estimated as the difference between peak groundwater levels and the extrapolated antecedent  
455 recession. The estimate of recharge from this method is sensitive to the estimate of the  
456 specific yield.  $S_y$  is assumed to be 0.1 which is close to the measured effective porosity of the  
457 Eastern View Formation (Love et al., 1993), and takes into account the presence of finer  
458 sized sediments such as silt and clay in the aquifer. Annual water table fluctuations are  
459 between 0.9 and 3.7 m across all bores, which for  $S_y$  values of 0.1, imply that  $R = 130$  to  $372$   
460  $\text{mm yr}^{-1}$  in 2012 (mean of  $200 \text{ mm yr}^{-1}$ ) and  $90$  to  $300 \text{ mm yr}^{-1}$  in 2013 (mean of  $164 \text{ mm yr}^{-1}$ ).  
461 This equates to between 11 and 32 % of rainfall in 2012 and 12 and 28 % of rainfall in  
462 2013. The bores are screened 11.2 to 42 m below the ground surface and thus these recharge  
463 estimates will be minima due to the attenuation of pressure variations with depth (Scanlon et  
464 al., 2002). Recharge estimates are also susceptible to the value of specific yield, particularly  
465 where the aquifer is composed of finer sized sediments such as silt and clay. Regardless,  
466 estimates using bore hydrographs indicate that significant groundwater recharge to the  
467 unconfined Eastern View aquifer in the valley occurs via direct infiltration of precipitation.

468

### 469 (5.3) $^{14}\text{C}$ ages

470 As groundwater in the Eastern View Formation contains dissolved oxygen and nitrate  
471 (Victorian Water Resources Data Warehouse, 2013),  $\delta^{13}\text{C}$  values are low, and there are no

472 reported occurrences of methane or coal seams within the Gellibrand River Catchment,  
 473 methanogenesis is unlikely to be a source of DIC. Likewise there are no obvious sources of  
 474 geogenic CO<sub>2</sub> in this area. Based on the major ion geochemistry, only minor calcite  
 475 dissolution occurs in the Eastern View Formation, which is to be expected as the Cenozoic  
 476 aquifers are siliceous and contain only minor carbonate minerals. While only minor carbonate  
 477 dissolution is likely, determination of groundwater residence times requires this to be taken  
 478 into account. If it is assumed that closed system dissolution of calcite in the aquifers is the  
 479 major process, the fraction of C derived from the soil zone (*q*) may be derived from the δ<sup>13</sup>C  
 480 values of DIC (δ<sup>13</sup>C<sub>DIC</sub>), carbonate (δ<sup>13</sup>C<sub>cc</sub>) and recharging water (δ<sup>13</sup>C<sub>r</sub>) via Eq.(2):

481

$$482 \quad q = \frac{\delta^{13}\text{C}_{DIC} - \delta^{13}\text{C}_{cc}}{\delta^{13}\text{C}_r - \delta^{13}\text{C}_{cc}} \quad (2)$$

483

484 (Clark & Fritz 1997). The calcite is assumed to have a δ<sup>13</sup>C of ~0‰ (Love et al., 1994;  
 485 Petrides and Cartwright, 2006) as is appropriate for marine sediments. δ<sup>13</sup>C<sub>r</sub> is calculated  
 486 from the δ<sup>13</sup>C of the soil carbon in the recharge zone. Pre-land clearing vegetation in  
 487 southeast Australia was dominated by eucalypts that have δ<sup>13</sup>C values of -30 to -27 ‰ (Quade  
 488 et al., 1995). Assuming a ~4 ‰ <sup>13</sup>C fractionation during outgassing (Cerling et al., 1991),  
 489 δ<sup>13</sup>C values of soil CO<sub>2</sub> would be -26 to -23 ‰ (average of -24.5 ‰). At 20 °C and pH 6.5,  
 490 δ<sup>13</sup>C<sub>r</sub> calculated from the fractionation data of Vogel et al. (1970) and Mook et al. (1974) is  
 491 ~ -20 ‰. Although the calculated δ<sup>13</sup>C<sub>r</sub> values require the pH and temperature of recharge  
 492 and the δ<sup>13</sup>C of the soil zone CO<sub>2</sub> to be estimated, they are similar to those from other studies  
 493 in southeast Australia and consistent with the predicted δ<sup>13</sup>C values of DIC in equilibrium  
 494 with calcite in the regolith (Quade et al., 1995; Cartwright, 2010). Calculated *q* values are  
 495 between 0.85 and 0.97 (Table 2), implying that only 10% to 15% of DIC in groundwater

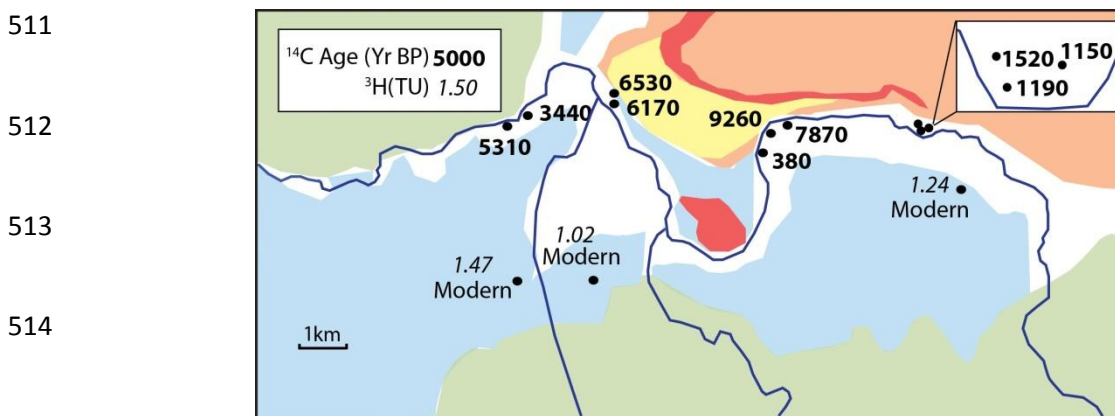
496 from the Eastern View formation is derived from calcite in the aquifer, this is similar to the  
 497 expected contribution of calcite dissolution in siliceous aquifers (Vogel et al., 1970) and  
 498 similar to other estimates from the Otway Basin (Love et al., 1994; Petrides and Cartwright,  
 499 2006).

500 Using the q values from Table 2,  $^{14}\text{C}$  ages (t) corrected for closed-system calcite dissolution  
 501 are calculated from Eq. (3); where  $a^{14}\text{C}$  is the activity of  $^{14}\text{C}$  in groundwater DIC, and  $a_o^{14}\text{C}$  is  
 502 the activity during recharge (assumed to be 100 pMC).

503

$$504 \quad t = -8376 \ln \left( \frac{a^{14}\text{C}}{q \cdot a_o^{14}\text{C}} \right) \quad (3)$$

505 Radiocarbon ages for groundwater in the Eastern View Formation range from 380 to 9260  
 506 years (Table 2) with the exception of bores 5k, 5l and 5m which have  $a^{14}\text{C} > 100$  pMC and  
 507 represent groundwater that has a component of water recharged during or after the  
 508 atmospheric nuclear tests in the 1950s to 1960s. The majority of  $^{14}\text{C}$  ages however, suggest  
 509 that groundwater in the valley, especially in the near-river environment has long residence  
 510 times (Fig. 7).



516 **Figure 7** – Groundwater residences times within the Gellibrand Valley. Residence times up to 9260  
 517 years are found in close proximity to the river. Modern local groundwaters with  $a^{14}\text{C} > 100$  pMC are  
 518 situated back on the floodplain. Data from Tables 1 and 2.

519 (5.4) <sup>3</sup>H Activities and Recharge Rates

520 With a shorter half-life, <sup>3</sup>H activities can infer the presence of modern groundwater. The  
521 water table fluctuations imply that the Gellibrand Valley receives considerable recharge year  
522 (90 to 370 mm yr<sup>-1</sup>), and although head gradients at nested sites are upwards implying that  
523 the valley is a groundwater discharge zone (Fig. 2b), these may be reversed during periods of  
524 high rainfall. If local recharge is significant in recharging the groundwater system across the  
525 valley, it would be expected that the groundwater would have relatively high <sup>3</sup>H activities.  
526 Recently-recharged groundwater in other Victorian catchments has <sup>3</sup>H activities up to 3.6 TU  
527 (Cartwright & Morgenstern, 2012).

528

529 <sup>3</sup>H activities across most of the groundwater from the Gellibrand Valley are negligible, and  
530 with <sup>14</sup>C ages of 380 to 9260 years, much of the groundwater is regional, originating from the  
531 Barongarook High. The exception to this is groundwater from the southern edge of the valley  
532 (Site 5) where the Eastern View Formation overlies the basement rock (Eumeralla Formation)  
533 and <sup>3</sup>H activities and <sup>14</sup>C activities are substantially higher than groundwater from sites 1 to 4.  
534 The mean residence times of water samples from the southern margin of the valley (Site 5)  
535 were evaluated from <sup>3</sup>H activities using the TracerLPM Excel workbook (Jurgens et al.,  
536 2012). As the aquifer is unconfined throughout the valley, and bore screens sample only part  
537 of the aquifer, the partial exponential model (PEM) is applied, with the PEM ratio calculated  
538 for bores 5k, 5l and 5k as the ratio of the unsampled thickness of the aquifer to the sampled  
539 thickness (Jurgens et al., 2012). A value of 2.7 TU was used to represent modern and pre-  
540 bomb pulse rainfall based on the <sup>3</sup>H activity of rainfall measured at Monash University and  
541 expected <sup>3</sup>H values in Southern Victoria (Tadros et al., 2014). For intervening years, the  
542 mean weighted average of <sup>3</sup>H activities in precipitation in Melbourne was extracted from the

543 International Atomic Energy Agency Melbourne record (International Atomic Energy  
544 Association, 2014). Calculated groundwater ages of 65 years (5k) 73 years (5l) and 59 years  
545 (5m) indicate that groundwater away from the river is modern and likely recharged from  
546 direct infiltration of precipitation. This supports  $\delta^{18}\text{O}$  and  $\delta^2\text{H}$  data which suggests that sites  
547 1 to 4 sample old, regional groundwater recharged on the Barongarook High, whilst site 5  
548 samples locally recharged groundwater within the valley. Although groundwater levels across  
549 sites 1 to 5 demonstrate annual recharge cycles, in the near-river environment (sites 1 to 4)  
550 much of the regional groundwater is from within 5 to 10 m of the water table, suggesting that  
551 any local recharge penetrates only to a limited depth, and does not mix with the bulk of the  
552 water in the Eastern View Formation. Conversely the high  $^3\text{H}$  activities and  $^{14}\text{C}$  activities at  
553 site 5, which occur in groundwater from depths of 21 – 42 m, imply that recharge to the  
554 deeper parts of the aquifer locally occurs at the southern edge of the floodplain.

555

556 The Gellibrand River has the potential to recharge regional groundwater during high river  
557 stages and episodic floods. Aquifer recharge from surface water can be assessed by  
558 combining data from groundwater EC values and  $^3\text{H}$  activities. The EC of river water varies  
559 between 120 and 200  $\mu\text{S cm}^{-1}$  and is lower than that of groundwater in the catchment  
560 throughout the year.  $^3\text{H}$  activities of river water are between 1.24 and 2.0 TU during baseflow  
561 conditions (Atkinson et al., 2013), and may be higher during high flow events as local  
562 modern rainfall (with  $^3\text{H}$  activities of 2.4 to 3.2 TU: Tadros et al., 2014) and relatively ‘young’  
563 water draining the upper catchment likely comprise a significant component of river flow at  
564 those times. Significant amounts of aquifer recharge through overbank events or bank  
565 exchange should result in groundwater with low EC values, and high  $^3\text{H}$  activities near the  
566 river. Except for in June 2012 when the bores were overtopped and a limited to response to  
567 high river flow events (June to July 2013), groundwater EC remains relatively constant



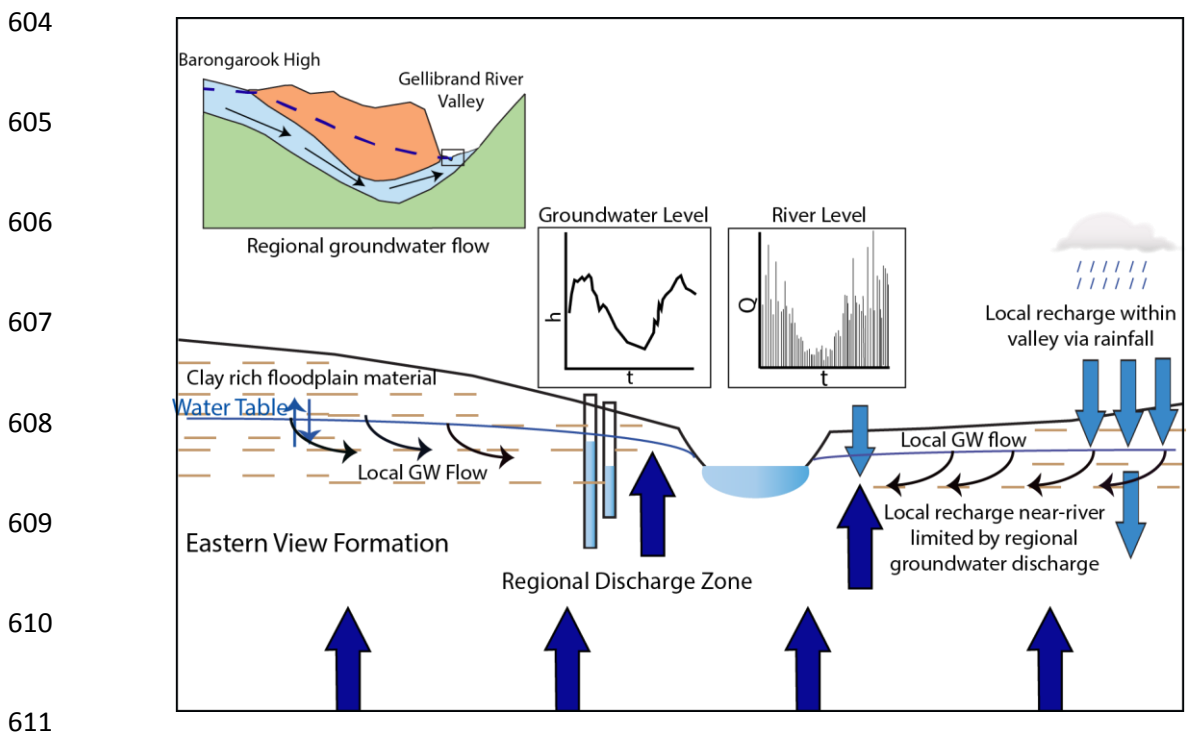
568 throughout the study period and there is only a minor inverse relationship with river height  
569 (Fig. 6). This indicates there is little exchange of river water to the depth of the aquifer  
570 sampled by the bores. Additionally the activities of  $^3\text{H}$  in near-river bores are negligible,  
571 again suggesting that recharge from the river does not penetrate more than a few metres into  
572 the adjacent aquifer. Thus, flow through the river bank or river flooding does not appear to be  
573 a significant mechanism of recharge in the Gellibrand Valley. Instead, with upward head  
574 gradients and evidence for limited recharge in the near-river environment, the river likely acts  
575 as a groundwater discharge zone for the majority of the year, supplied by a combination of  
576 regional groundwater from the Barongarook High and local groundwater recharged within  
577 the valley.

578

#### 579 (5.5) Groundwater Flowpaths and Conceptual Model

580 Radiocarbon ages are up to 10 ka implying that the groundwater in the Gellibrand Valley has  
581 a long residence time; in turn this implies that the area is a regional discharge zone. Most of  
582 the groundwater originates on the Barongarook High, and this region potentially provides a  
583 substantial proportion of baseflow to the Gellibrand River. The large range of  $^{14}\text{C}$  ages in the  
584 Gellibrand Valley is a likely result of heterogeneous geology, where the presence of low  
585 hydraulic conductivity sediments such as silt and clays in the Eastern View Formation lead to  
586 variable velocities along groundwater flowpaths. Groundwater travel times may also be  
587 determined using the present day hydraulic gradients. From Darcy's law and assuming a  
588 porosity of 0.1 (Love et al., 1994) and a hydraulic conductivity of 0.2 to 2 m day $^{-1}$  (Love et  
589 al., 1993) calculated travel times are between 1000 and 10 000 years, which are similar to  
590 those implied by the  $^{14}\text{C}$  ages. This and the depleted stable isotope signature of groundwater  
591 samples from sites 1 to 4 supports the idea that groundwater in the valley is predominantly

592 regional groundwater derived by recharge on the Barongarook High. The high  $^3\text{H}$  activities in  
 593 groundwater bores from site 5 situated away from the river imply local recharge via  
 594 precipitation recharges the aquifer to depths of 21 to 42 m at the southern edge of the  
 595 floodplain. However for the most-part, shallow groundwater in the Gellibrand Valley,  
 596 including in the near-river environment is predominantly regional groundwater. Though  
 597 groundwater elevations display clear annual cycles and winter months are punctuated by high  
 598 river flow, localised recharge from both of these processes combined is stored in the upper 10  
 599 m of the aquifer. The infiltration of precipitation within the Gellibrand Valley is likely  
 600 limited by the presence of silts and clays on the floodplain and riverbanks. This is coupled  
 601 with strong upwards hydraulic gradients in the Eastern View Formation, driven by regional  
 602 groundwater flow from the Barongarook High, which ensure that recharge in the near-river  
 603 environment does not penetrate deep within the aquifer (Fig. 8).

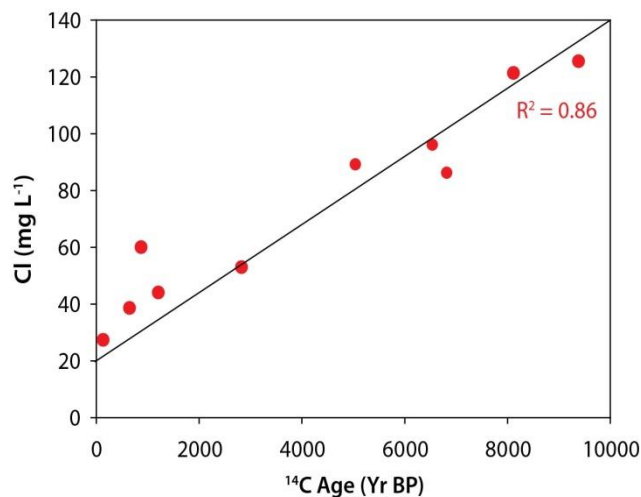


612 **Figure 8** – Groundwater flow conceptualisation in the Gellibrand Valley. Though appreciable  
 613 amounts of recharge are estimated from bore hydrographs and high river flows, the depth to which  
 614 recharging waters infiltrate into the Eastern View Formation (downward leakage) is limited by strong  
 615 upward head gradients, and a floodplain which consists of appreciable amounts of silt and clay.

616 (5.6)  $^{14}\text{C}$  ages & Cl

617 The good correlation of a  $^{14}\text{C}$  with chloride implies that chloride concentrations correspond to  
618 groundwater age (Fig. 9). Correlations between  $^{14}\text{C}$  and Cl have also been documented in  
619 groundwater from the Eastern View Formation in other regions of the Otway Basin (Love et  
620 al., 1994). In assessing this relationship, chloride sources must be considered. That the Cl/Br  
621 ratios in the groundwater are similar to those of rainfall preclude significant halite dissolution  
622 by the groundwater from the Eastern View Formation, and there are no extensive occurrences  
623 of halite in the aquifer matrix.

624



625

626

627

628

629

630 **Figure 9** –  $^{14}\text{C}$  age v Cl.  $^{14}\text{C}$  ages are taken from the calcite corrected ages in *Table 1*

631

632 We propose three possible explanations of this trend. Firstly, the relationship between a  $^{14}\text{C}$   
633 and Cl may be explained by mixing of low salinity groundwater that is locally recharged  
634 within the valley (Site 5) and high salinity regional groundwater from the Barongarook High  
635 (Sites 1 to 4). However, groundwater samples from site 5 which have high a  $^{14}\text{C}$  and low Cl  
636 also have high  $^3\text{H}$  activities (0.99 to 1.47 TU) suggesting if mixing has occurred it must do so  
637 at a very slow rate otherwise the resultant groundwater (Sites 1 to 4) would be expected to

638 contain measurable  $^3\text{H}$ . This implies that mixing between the shallow groundwater system  
639 and the deeper groundwater is limited.

640

641 It is possible that the Cl concentrations in groundwater preserve a record of climate  
642 variability. In the Otway Basin Love et al. (1994) report a decrease in Cl concentrations in  
643 groundwater recharged between 18 and 10 ka, followed by an increase in Cl concentrations in  
644 groundwater recharged from 10 ka to the present day, which they attribute to increased  
645 evapotranspiration rates during a warming Holocene climate. However, in this study  
646 decreasing Cl concentrations with increasing  $a^{14}\text{C}$  would imply that recharge rates on the  
647 Barongarook high increased from 10,000 years BP to the present, which is not likely given  
648 the warming trend over that period.

649

650 It is more likely that the correlation between  $a^{14}\text{C}$  and Cl concentrations reflects spatially  
651 variable recharge on the Barongarook High due to the heterogeneous sediments within the  
652 Eastern View Formation. Evapotranspiration during recharge is commonly the dominant  
653 process in determining the salinity of groundwater in SE Australia (Herczeg et al., 2001).  
654 Low recharge rates result in higher degrees of evapotranspiration and higher salinity  
655 groundwater, and the resultant correlation between Cl concentrations and  $^{14}\text{C}$  ages has been  
656 noted in other catchments (Leaney et al., 2003; Cartwright et al., 2006). Variable recharge  
657 rates could result in a wide range of recharge ages in the Gellibrand Valley, with the high Cl  
658 low  $a^{14}\text{C}$  groundwater being derived from regions with locally low recharge rates. Regardless  
659 of which model is correct, the chloride measurements provide a useful first order estimate of  
660 groundwater residence times.

661 **(6) Conclusion**

662 Though widely available water-table measurements offer an insight into recharge, the  
663 dynamics of groundwater flow systems and recharge patterns can only be fully understood  
664 when combined with geochemical data, in particular radiogenic tracers such as  $^3\text{H}$  and  $^{14}\text{C}$ .  
665 These can be used to assess the importance of recharge and discharge in aquifer windows,  
666 which in turn defines groundwater pathways and allows the potential fate of pollutants to be  
667 assessed. Here shallow (11 to 42 m) groundwater bores indicate a significant amount of  
668 recharge occurs in the Gellibrand River Valley (90 to 370 mm yr<sup>-1</sup>). However, the  
669 groundwater at 5 to 10 m below the water table has  $^{14}\text{C}$  ages between 350 and 10,000 years,  
670 and below detection  $^3\text{H}$  activities. Furthermore, there is no indication of water from the river  
671 penetrating more than ~10 m following flood events. In the Gellibrand River Valley,  
672 outcropping aquifer sediments act as a regional discharge zone. Upwards head gradients are  
673 maintained for long periods of time and aided by the presence of silts and clays on the  
674 floodplain, this limits the depth to which diffuse and localised recharge (via over-bank events  
675 and bank exchange) penetrate the aquifer.

676

677 There is most likely a shallow local flow system within the Gellibrand River Valley that has  
678 limited connectivity with the deeper groundwater, particularly in the near-river environment.  
679 This potentially limits the spread of pollutants such as nitrate and pesticides that may derive  
680 from the agricultural activities into the regional groundwater. Future land-use, climate change  
681 or groundwater exploitation that occurs on the Barongarook High or in the Gellibrand River  
682 Catchment is likely to affect both the chemistry of groundwater and groundwater fluxes to the  
683 Gellibrand River, highlighting the importance of protecting regional recharge zones.

684

685 **Acknowledgements**

686

687 We would like to thank colleagues who assisted in labarotary analysis. In particular, Massimo  
688 Raveggi and Rachele Pierson (Monash University) for stable isotope, anion and cation  
689 analyses, and Simon Varley (ANSTO) for 14C determinations.

690

691 **References**

692

693 Alley, W.M., Healy, R.W., LaBaugh J.W., and Reilly, T.E.: Flow and storage in groundwater  
694 systems. (Review: hydrology). Science, 296: 1985-1990 DOI:10.1126/science.106712,  
695 2002.

696

697 Aravena, R., Leonard, I., Wassenaar, L., and Plummer, N.: Estimating <sup>14</sup>C Groundwater  
698 Ages in a Methanogenic Aquifer. Water Resour Res, 9: 2307-2317. DOI:  
699 10.1029/95WR01271, 1995.

700

701 Atkinson, A.P., Cartwright, I., Gilfedder, B.S., Hofmann, H., Unland, N.P., Cendón, D.I., and  
702 Chisari, R.: A multi-tracer approach to quantifying groundwater inflows to an upland  
703 river; assessing the influence of variable groundwater chemistry. Hydrol Process.  
704 Available Online. DOI: 10.1002/hyp.10122, 2013.

705

706 Bennetts, D.A., Webb, J.A., Stone, D.J.M., and Hill, D.M.: Understanding the salinisation  
707 process for groundwater in an area of south-eastern Australia, using hydrochemical  
708 and isotopic evidence. J Hydrol, 323: 178-192. DOI:  
709 <http://dx.doi.org/10.1016/j.jhydrol.2005.08.023>, 2006.

710

711 Bertrand, G., Celle-Jeanton, H., Loock, S., Huneau, F., Lavastre, V.: Contribution of  
712  $\delta^{13}\text{C}$  and  $\text{PCO}_2$  eq measurements to the understanding of groundwater  
713 mineralization and carbon patterns in volcanic aquifers. Application to Argnat Basin  
714 (Massif Central). *Aq. Geochem.* 19 (2): 147-171. DOI: 10.1007/s10498-012-9185-0,  
715 2013.

716

717 Bethke, C.M. and Johnson, T.M.: Groundwater Age and Groundwater Age Dating. *Annual*  
718 *Review of Earth Planet Sc Lett*, 36: 121-152. DOI:  
719 0.1146/annurev.earth.36.031207.124210, 2008.

720

721 Blackburn, G. and McLeod, S.: Salinity of atmospheric precipitation in the Murray-Darling  
722 drainage division, Australia. *Soil Research*, 21: 411-434. DOI:  
723 <http://dx.doi.org/10.1071/SR9830411>, 1983.

724

725 Böhlke, J.K. and Denver, J.M.: Combined Use of Groundwater Dating, Chemical, and  
726 Isotopic Analyses to Resolve the History and Fate of Nitrate Contamination in Two  
727 Agricultural Watersheds, Atlantic Coastal Plain, Maryland. *Water Resour Res*, 31:  
728 2319-2339. DOI: 10.1029/95wr01584, 1995.

729

730 Böhlke, J.K.: Groundwater recharge and agricultural contamination. *Hydrogeol J*, 10: 153-  
731 179. DOI: 10.1007/s10040-001-0183-3, 2002.

732

733 Briguglio, D., Kowalczyk, J., Stilwell, J.D., Hall, M., and Coffa, A.: Detailed  
734 paleogeographic evolution of the Bass Basin: Late Cretaceous to present. *Aust Journal*  
735 *Earth Sci*, 60: 719-734. DOI: 10.1080/08120099.2013.826282, 2013.

736

737 Bureau of Meteorology, 2013. Commonwealth of Australia Bureau of Meteorology.  
738 <http://www.bom.gov.au>, last access: 14 January 2014.

739

740 Campana, M.E. and Simpson, E.S.: Groundwater residence times and recharge rates using a  
741 discrete-state compartment model and  $^{14}\text{C}$  data. *J Hydrol*, 72: 171-185. DOI:  
742 [http://dx.doi.org/10.1016/0022-1694\(84\)90190-2](http://dx.doi.org/10.1016/0022-1694(84)90190-2), 1984.

743

744 Cardenas, M.B.: Potential contribution of topography-driven regional groundwater flow to  
745 fractal stream chemistry: Residence time distribution analysis of Tóth flow. *Geophys*  
746 *Res Lett*, 34: L05403. DOI: 10.1029/2006gl029126, 2007.

747

748 Cartwright, I., Weaver, T.R., and Fifield, L.K.: Cl/Br ratios and environmental isotopes as  
749 indicators of recharge variability and groundwater flow: An example from the  
750 southeast Murray Basin, Australia. *Chem. Geol*, 231: 38-56. DOI:  
751 <http://dx.doi.org/10.1016/j.chemgeo.2005.12.009>, 2006.

752

753 Cartwright, I. and Morgenstern, U.: Constraining groundwater recharge and the rate of  
754 geochemical processes using tritium and major ion geochemistry: Ovens catchment,  
755 southeast Australia. *J Hydrol*, 475: 137-149. DOI:  
756 <http://dx.doi.org/10.1016/j.jhydrol.2012.09.037>, 2012.

757

758 Cartwright, I., Weaver, T.R., Cendón, D.I., Fifield, L.K., Tweed, S.O., Petrides, B., and  
759 Swane I.: Constraining groundwater flow, residence times, inter-aquifer mixing, and  
760 aquifer properties using environmental isotopes in the southeast Murray Basin,  
761 Australia. *Appl Geochem*, 27: 1698-1709. DOI:  
762 <http://dx.doi.org/10.1016/j.apgeochem.2012.02.006>, 2012.

763

764 Cartwright, I., Fifield, L.K., and Morgenstern, U.: Using  $^3\text{H}$  and  $^{14}\text{C}$  to constrain the degree of  
765 closed-system dissolution of calcite in groundwater. *App Geochem*, 32: 118-128. DOI:  
766 <http://dx.doi.org/10.1016/j.apgeochem.2012.10.023>, 2013.



767

768 Cendón, D.I., Larsen, J.R., Jones, B.G., Nanson, G.C., Rickleman, D., Hankin, S.I., Pueyo,  
769 J.J., and Maroulis, J.: Freshwater recharge into a shallow saline groundwater system,  
770 Cooper Creek floodplain, Queensland, Australia. *J Hydrol*, 392: 150-163. DOI:  
771 <http://dx.doi.org/10.1016/j.jhydrol.2010.08.003>, 2010.

772 Cendón, D.I., Hankin, S.I., Williams, J.P., Van Der Ley, M., Peterson, M., Hughes, C.E.,  
773 Meredith, K., Graham, I.T., Hollins, S.E., Levchenko, V., and Chisari, R.:  
774 Groundwater residence time in a dissected and weathered sandstone plateau: Kulnura-  
775 Mangrove Mountain aquifer, NSW, Australia. *Aust J of Earth Sci*, 1-25  
776 <http://dx.doi.org/10.1080/0812099.2014.894628>, 2014.

777

778 Cerling, T.E., Solomon, D.K., Quade, J., and Bowman, J.R.: On the isotopic composition of  
779 carbon in soil carbon dioxide. *Geochim Cosmochim Ac*, 55: 3403-3405. DOI:  
780 [http://dx.doi.org/10.1016/0016-7037\(91\)90498-T](http://dx.doi.org/10.1016/0016-7037(91)90498-T), 1991.

781

782 Chen, X. and Chen, X.: Stream water infiltration, bank storage, and storage zone changes due  
783 to stream-stage fluctuations. *J Hydrol*, 280: 246-264. DOI:  
784 [http://dx.doi.org/10.1016/S0022-1694\(03\)00232-4](http://dx.doi.org/10.1016/S0022-1694(03)00232-4), 2003.

785

786

787 Clark, I.D. and Fritz, P.: *Environmental Isotopes in Hydrogeology*. Lewis, New York, USA,  
788 1997.

789

790 Cook, P., Herczeg, A., and Kalin, R.: Radiocarbon Dating of Groundwater Systems. In:  
791 *Environmental Tracers in Subsurface Hydrology*, Springer US, pp: 111-144, 2000.

792

793 Cook, P.G. and Robinson, N.I.: Estimating groundwater recharge in fractured rock from  
794 environmental <sup>3</sup>H and <sup>36</sup>Cl, Clare Valley, South Australia. *Water Res Res*, 38: 11-11-  
795 11-13. DOI: 10.1029/2001wr000772, 2002.

796

797 Coplen, T.B.: Normalization of oxygen and hydrogen isotope data. *Chem. Geol.*, 72: 293-297.  
798 DOI: 10.1016/0168-9622(88)90042-5, 1988.

799 Dansgaard, W.: Stable isotopes in precipitation. *Tellus.*, 16 (4): 436-468.  
800 DOI:10.1111/j.2153-3490.1964.tb00181.x, 1964.

801

802 Doble, R.B.P., McCallum, J., and Cook, P.: An analysis of river bank slope and unsaturated  
803 flow effect on bank storage. *Groundwater*, 50: 77-86. DOI: 0.1111/j.1745-  
804 6584.2011.00821.x, 2012.

805

806 Edmunds, W.M., Carrillo-Rivera, J.J., and Cardona, A.: Geochemical evolution of  
807 groundwater beneath Mexico City. *J Hydrol*, 258: 1-24. DOI:  
808 [http://dx.doi.org/10.1016/S0022-1694\(01\)00461-9](http://dx.doi.org/10.1016/S0022-1694(01)00461-9), 2002.

809

810 Fink, D., Hotchkis, M., Hua, Q., Jacobsen, G., Smith, A.M., Zoppi, U., Child, D., Mifsud, C.,  
811 van der Gaast, H., Williams, A., and Williams, M.: The ANTARES AMS facility at  
812 ANSTO. *Nuclear Instruments and Methods in Physics Research B* 223-224, 109-115,  
813 2004.

814

815 Foster, S.S.D., and Chilton, P.J.: Groundwater: the processes and global significance of  
816 aquifer degradation. *Philosophical Transactions of the Royal Society of London*  
817 *Series B-Biological Sciences*, 358: 1957-1972. DOI: 10.1098/rstb.2003.1380, 2003.

818

819 Frederico, C., Aiuppa, A., Allad, P., Bellomo, S., Jean-Baptiste, P., Parello, F., Valenza, M.:  
820 Magma-derived gas influx and water-rock interactions in the volcanic aquifer of Mt  
821 Vesuvius, Italy. *Geochim. Cosmochim. Acta*, 66(6): 963-981, 2002.

822

823 Frisbee, M.D., Wilson, J.L., Gomez-Velez, J.D., Phillips, F.M., and Campbell, A.R.: Are we  
824 missing the tail (and the tale) of residence time distributions in watersheds? *Geophys*  
825 *Res Lett*, 40: 4633-4637. DOI: 10.1002/grl.50895, 2013.

826 Gardner, W.P., Harrington, G.A., Solomon, D.K., and Cook, P.G.: Using terrigenic  $^4\text{He}$  to  
827 identify and quantify regional groundwater discharge to streams. *Water Resour Res*,  
828 47: W06523. DOI: 10.1029/2010wr010276, 2011.

829

830 Goderniaux, P., Davy, P., Bresciani, E., de Dreuzy, J.R., and Le Borgne, T.: Partitioning a  
831 regional groundwater flow system into shallow local and deep regional flow  
832 compartments. *Water Resour Res*, 49: 2274-2286. DOI: 10.1002/wrcr.20186, 2013.

833

834 Han, L.F. and Plummer, L.N.: Revision of Fontes & Garnier's model for the initial  $^{14}\text{C}$   
835 content of dissolved inorganic carbon used in groundwater dating. *Chem. Geol.*, 351:  
836 105-114. DOI: <http://dx.doi.org/10.1016/j.chemgeo.2013.05.011>, 2013.

837

838 Herczeg, A.L., Dogramaci, S.S., and Leaney, F.W.J.: Origin of dissolved salts in a large,  
839 semi-arid groundwater system: Murray Basin, Australia. *Mar. Freshw. Res.*, 52: 41-52.  
840 DOI: <http://dx.doi.org/10.1071/MF00040>, 2001.

841

842 Hilscherova, K., Dusek, L., Kubik, V., Cupr, P., Hofman, J., Klanova, J., and Holoubek, I.:  
843 Redistribution of organic pollutants in river sediments and alluvial soils related to  
844 major floods. *Journal of Soils and Sediments*, 7: 167-177. DOI:  
845 10.1065/jss2007.04.222, 2007.

846

847 Hortle, A., de Caritat, P., Stalvies, C., and Jenkins, C.: Groundwater monitoring at the Otway  
848 project site, Australia. Energy Procedia, 4: 5495-5503. DOI:  
849 <http://dx.doi.org/10.1016/j.egypro.2011.02.535>, 2011.

850

851 Hughes, C.E. and Crawford, J.: A new precipitation weighted method for determining the  
852 meteoric water line for hydrological applications demonstrated using Australian and  
853 global GNIP data. J Hydrol, 464: 344-351. DOI:  
854 <http://dx.doi.org/10.1016/j.jhydrol.2012.07.029>, 2012.

855

856 Jurgens B.C., Böhlke J.K., Eberts S.M.: TracerLPM (Version 1): An Excel® workbook for  
857 interpreting groundwater age distributions from environmental tracer data: U.S.  
858 Geological Survey Techniques and Methods Report 4- F3, 60p, 2012.

859

860 Krüger, F., Meissner, R., Gröngröft, A., and Grunewald, K.: Flood Induced Heavy Metal and  
861 Arsenic Contamination of Elbe River Floodplain Soils. Acta hydroch hydrob, 33:  
862 455-465. DOI: 10.1002/aheh.200400591, 2005.

863

864 Leaney, F.W., Herczeg, A.K., Walker, G.R.: Stable isotope geochemistry of ground and  
865 surface waters associated with undisturbed massive sulphide deposits; constraints on  
866 origin of waters and water-rock reactions. Chemical Geology, 2006.

867

868 Leonard, J., Lakey, R., and Cumming, S.: Gellibrand groundwater investigation interim  
869 report. Geologic Survey of Victoria. Department of Minerals and Energy.  
870 Unpublished Report, 1981

871

872 Le Gal La Salle, C., Marlin, C., Leduc, C., Taupin, J.D., Massault, M., and Favreau, G.:  
873 Renewal rate estimation of groundwater based on radioactive tracers (<sup>3</sup>H, <sup>14</sup>C) in an

874 unconfined aquifer in a semi-arid area, Iullemeden Basin, Niger. J Hydrol, 254: 145-  
875 156. DOI: [http://dx.doi.org/10.1016/S0022-1694\(01\)00491-7](http://dx.doi.org/10.1016/S0022-1694(01)00491-7), 2001.

876

877 Love, A.J., Herczeg, A.L., Armstrong, D., Stadter, F., and Mazor, E.: Groundwater flow  
878 regime within the Gambier Embayment of the Otway Basin, Australia: evidence from  
879 hydraulics and hydrochemistry. J Hydrol, 143: 297-338. DOI:  
880 [http://dx.doi.org/10.1016/0022-1694\(93\)90197-H](http://dx.doi.org/10.1016/0022-1694(93)90197-H), 1993.

881 Love, A.J., Herczeg, A.L., Leaney, F.W., Stadter, M.F., Dighton, J.C., and Armstrong, D.:  
882 Groundwater residence time and palaeohydrology in the Otway Basin, South  
883 Australia:  $^2\text{H}$ ,  $^{18}\text{O}$  and  $^{14}\text{C}$  data. J Hydrol, 153: 157-187. DOI:  
884 [http://dx.doi.org/10.1016/0022-1694\(94\)90190-2](http://dx.doi.org/10.1016/0022-1694(94)90190-2), 1994.

885

886 Manning, A.H., Clark, J.F., Diaz, S.H., Rademacher, L.K., Earman, S., and Plummer, N.L.:  
887 Evolution of groundwater age in a mountain watershed over a period of thirteen years.  
888 J Hydrol, 460: 13-28. DOI: <http://dx.doi.org/10.1016/j.jhydrol.2012.06.030>, 2012.

889

890 Mazor, E., and Nativ, R.: Hydraulic calculation of groundwater flow velocity and age:  
891 examination of the basic premises. J Hydrol, 138: 211-222. DOI:  
892 [http://dx.doi.org/10.1016/0022-1694\(92\)90165-R](http://dx.doi.org/10.1016/0022-1694(92)90165-R), 1992.

893

894 McCallum, J.L., Cook, P.G., Brunner, P., and Berhane, D.: Solute dynamics during bank  
895 storage flows and implications for chemical base flow separation. Water Resour. Res.,  
896 46: W07541. DOI: 10.1029/2009wr008539, 2010.

897

898 McDonnell, J.J., McGuire, K., Aggarwal, P., Beven, K.J., Biondi, D., Destouni, G., Dunn, S.,  
899 Kirchner, J.A., Kraft, P., Lyon, S., Maloszewski, P., Newman, B., Pfister, L., Rinaldo,  
900 A., Rodhe, A., Sayama, T., Seibert, J., Solomon, K., Soulsby, C., Stewart, M.,  
901 Tetzlaff, D., Tobin, C., Troch, P., Weiler, M., Western, A., Wörman, A., and Wrede,

902 S.: How old is streamwater? Open questions in catchment transit time  
903 conceptualization, modelling and analysis. *Hydrol Process*, 24: 1745-1754. DOI:  
904 10.1002/hyp.7796, 2010.

905

906 Meredith, K.T., Cendón, D.I., Pigois, J-P., Hollins, S.E., and Jacobsen, G.: Using  $^{14}\text{C}$  and  $3\text{H}$   
907 to delineate a recharge 'window' into the Perth Basin aquifers, North Gnamptara  
908 groundwater system, Western Australia. *Sci Total Environ*, 414, 456-469, 2012.

909 Michel, R.L.: Tritium hydrology of the Mississippi River basin. *Hydrol Process*, 18: 1255-  
910 1269. DOI: 10.1002/hyp.1403, 2004.

911

912 Moench, A.F. and Barlow, P.M.: Aquifer response to stream-stage and recharge variations. I.  
913 Analytical step-response functions. *J Hydrol*, 230: 192-210. DOI:  
914 [http://dx.doi.org/10.1016/S0022-1694\(00\)00175-X](http://dx.doi.org/10.1016/S0022-1694(00)00175-X), 2000.

915

916 Mook, W.G., Bommerson, J.C., and Staverman, W.H.: Carbon isotope fractionation between  
917 dissolved bicarbonate and gaseous carbon dioxide. *Earth Planet Sc Lett*, 22: 169-176.  
918 DOI: [http://dx.doi.org/10.1016/0012-821X\(74\)90078-8](http://dx.doi.org/10.1016/0012-821X(74)90078-8), 1974.

919

920 Morgenstern, U. and Taylor, C.B.: Ultra low-level tritium measurement using electrolytic  
921 enrichment and LSC. *Isot environ and health s*, 45(2) 96-117, 2009.

922

923 Morgenstern, U. Stewart, M.K., and Stenger, R.: Dating of streamwater using tritium in a  
924 post nuclear bomb pulse world: continuous variation of mean transit time with  
925 streamflow. *Hydrol. Earth Syst. Sci.*, 14: 2289-2301. DOI: 10.5194/hess-14-2289-  
926 2010.

927

928 Muennich, K.O.: Messung des <sup>14</sup>C-Gehaltes von hartem Grundwasser. Naturwissenschaften  
929 34, 32-33, 1957.

930

931 Neklapilova, B.: Conductivity measurements and large volumes distillation of samples for  
932 Tritium analysis. ANSTO internal guideline. Technical Report ENV-I-070-002,  
933 ANSTO – Institute for Environmental Research, Australia, 2008a.

934 Neklapilova, B.: Electrolysis and small volume distillation of samples for tritium activity  
935 analysis, ANSTO internal guideline. Technical Report ENV-I-070-003, ANSTO –  
936 Institute for Environmental Research, Australia, 2008b.

937

938 Newsom, J.M. and Wilson, J.L.: Flow of Ground Water to a Well Near a Stream – Effect of  
939 Ambient Ground-Water Flow Direction. Ground Water, 26: 703-711. DOI:  
940 10.1111/j.1745-6584.1988.tb00420.x, 1988.

941

942 Payton Gardner, W., Susong, D.D., Kip Solomon, D., and Heasler, H.: Snowmelt hydrograph  
943 interpretation: Revealing watershed scale hydrologic characteristics of the  
944 Yellowstone volcanic plateau. J Hydrol, 383: 209-222. DOI:  
945 <http://dx.doi.org/10.1016/j.jhydrol.2009.12.037>, 2010.

946

947 Petrides, B. and Cartwright, I.: The hydrogeology and hydrogeochemistry of the Barwon  
948 Downs Graben aquifer, southwestern Victoria, Australia. Hydrogeol J, 14: 809-826.  
949 DOI: 10.1007/s10040-005-0018-8, 2006.

950

951 Post, V.E.A., Vandenbohede, A., Werner, A.D., Maimun, S., and Teubner, M.D.:  
952 Groundwater ages in coastal aquifers. *Adv in Water Resour*, 57: 1-11. DOI:  
953 <http://dx.doi.org/10.1016/j.advwatres.2013.03.011>, 2013.

954

955 Quade, J., Chivas, A.R., and McCulloch, M.T.: Strontium and carbon isotope tracers and the  
956 origins of soil carbonate in South Australia and Victoria. *Palaeogeogr Palaeocl*, 113:  
957 103-117. DOI: [http://dx.doi.org/10.1016/0031-0182\(95\)00065-T](http://dx.doi.org/10.1016/0031-0182(95)00065-T), 1995.

958

959 Reilly, T.E., Plummer, L.N., Phillips, P.J., and Busenberg, E.: The use of simulation and  
960 multiple environmental tracers to quantify groundwater flow in a shallow aquifer.  
961 *Water Resour Res*, 30: 421-433. DOI: 10.1029/93wr02655, 1994.

962

963 Samborska, K., Rózkowski, A., and Małozzewski, P.: Estimation of groundwater residence  
964 time using environmental radioisotopes ( $^{14}\text{C}$ , T) in carbonate aquifers, southern  
965 Poland. *Isot Environ Healt St*, 49: 73-97. DOI: 10.1080/10256016.2012.677041, 2012.

966

967 Scanlon, B., Healy, R., and Cook, P.: Choosing appropriate techniques for quantifying  
968 groundwater recharge. *Hydrogeol J*, 10: 18-39. DOI: 10.1007/s10040-001-0176-2,  
969 2002.

970

971 Shentsis, I. and Rosenthal, E.: Recharge of aquifers by flood events in an arid region. *Hydrol*  
972 *Process*17: 695-712. DOI: 10.1002/hyp.1160, 2003.

973

974 Sklash. M.G. and Farvolden, R.N.: The role of groundwater in storm runoff. *J Hydrol*, 43: 45-  
975 65. DOI: [http://dx.doi.org/10.1016/0022-1694\(79\)90164-1](http://dx.doi.org/10.1016/0022-1694(79)90164-1), 1979.

976



977 Smerdon, B.D., Payton Gardner, W., Harrington, G.A., and Tickell, S.J.: Identifying the  
978 contribution of regional groundwater to the baseflow of a tropical river (Daly River,  
979 Australia). J Hydrol, 464-465: 107-115. DOI:  
980 <http://dx.doi.org/10.1016/j.jhydrol.2012.06.058>, 2012.

981

982 Stewart, M.K.: A 40-year record of carbon-14 and tritium in the Christchurch groundwater  
983 system, New Zealand: Dating of young samples with carbon-14. J Hydrol, 430: 50-68.  
984 DOI: <http://dx.doi.org/10.1016/j.jhydrol.2012.01.046>, 2012.

985

986 Stichler, W., Maeszewski, P., and Moser, H.: Modelling of river water infiltration using  
987 oxygen-18 data. J Hydrol, 83: 355-365. DOI: [http://dx.doi.org/10.1016/0022-  
988 1694\(86\)90161-7](http://dx.doi.org/10.1016/0022-1694(86)90161-7), 1986.

989

990 Stuvier, M. And Polach, H.A.: Reporting of <sup>14</sup>C data. Radiocarbon, 19: 355-363, 1977.

991

992 Stuyfzand, P.J.: Hydrology and water quality aspects of rhine bank groundwater in The  
993 Netherlands. J Hydrol, 106: 341-363. DOI: [http://dx.doi.org/10.1016/0022-  
994 1694\(89\)90079-6](http://dx.doi.org/10.1016/0022-1694(89)90079-6), 1989.

995

996 Tadros, C.V., Hughes, C.E., Crawford, J., Hollins, S.E., and Chisari, R.: Tritium in Australian  
997 Precipitation: a 50 Year Record. J Hydrol. DOI:  
998 <http://dx.doi.org/10.1016/j.jhydrol.2014.03.031>, 2014.

999

1000 Tesoriero, A.J., Spruill, T.B., Mew, H.E., Farrell, K.M., and Harden, S.L.: Nitrogen transport  
1001 and transformations in a coastal plain watershed: Influence of geomorphology on flow  
1002 paths and residence times. Water Resour Res, 41: W02008. DOI:  
1003 10.1029/2003wr002953, 2005.

1004

1005 Tóth, J.: A theoretical analysis of groundwater flow in small drainage basins. *J Geophys Res*,  
1006 68: 4795-4812. DOI: 10.1029/JZ068i016p04795, 1963.

1007

1008

1009 Unland, N.P., Cartwright, I., Cendón, D.I., and Chisari, R.: Residence times and mixing of  
1010 water in river banks: implications for recharge and groundwater &ndash; surface  
1011 water exchange. *Hydrol. Earth Syst. Sci. Discuss.*, 11: 1651-1691. DOI:  
1012 10.5194/hessd-11-1651-2014, 2014.

1013

1014 Van den Berg, A.H.M., Rock unit names in western Victoria, Seamless Geology Project.  
1015 Geological Survey of Victoria Report 130. GeoScience Victoria, State of Victoria,  
1016 Department of Primary Industries, 2009.

1017

1018 Victorian Water Resources Data Warehouse: Victorian Department of Sustainability and  
1019 Environment Water Resources Data Warehouse, available at  
1020 <http://www.vicwaterdata.net>, last access: January 2014.

1021

1022 Vogel, J.C., Grootes, P.M., and Mook, W.G.: Isotopic fractionation between gaseous and  
1023 dissolved carbon dioxide. *Z. Physik*, 230: 225-238. DOI: 10.1007/bf01394688, 1970.

1024

1025 Vogel, J.C., Thilo, L., and Van Dijken, M.: Determination of groundwater recharge with  
1026 tritium. *J Hydrol*, 23: 131-140. DOI: [http://dx.doi.org/10.1016/0022-1694\(74\)90027-4](http://dx.doi.org/10.1016/0022-1694(74)90027-4),  
1027 1974.

1028

1029 Vogt, T., Hoehn, E., Schneider, P., Freund, A., Schirmer, M., and Cirpka, O.A.: Fluctuations  
1030 of electrical conductivity as a natural tracer for bank filtration in a losing stream. *Adv*

1031 Water Resour, 33: 1296-1308. DOI:  
1032 <http://dx.doi.org/10.1016/j.advwatres.2010.02.007>, 2010.  
1033  
1034 Wigley, T.M.L.: Carbon 14 dating of groundwater from closed and open systems. Water  
1035 Resour Res, 11: 324-328. DOI: 10.1029/WR011i002p00324, 1975.  
1036  
1037 Zhai, Y., Wang, J., Teng, Y., and Zuo, R.: Hydrogeochemical and isotopic evidence of  
1038 groundwater evolution and recharge in aquifers in Beijing Plain, China.  
1039 Environmental Earth Sciences, 69: 2167-2177. DOI: 10.1007/s12665-012-2045-9,  
1040 2013.

**Table 1** – Screen depth, Cl, <sup>18</sup>O, <sup>2</sup>H, <sup>13</sup>C, a<sup>14</sup>C and <sup>3</sup>H activities of groundwater samples. <sup>a</sup>Refers to bore name on the Victorian Water Resources Data Warehouse. <sup>b</sup> Measured as depth to the middle of the well screen. <sup>c</sup><sup>3</sup>H activities that are below detection.

Sample No.	Screen Depth (m)	EC (µS cm <sup>-1</sup> )	Cl	Br	Na	Ca	Mg	K	HCO <sub>3</sub> <sup>-</sup>	SO <sub>4</sub> <sup>2-</sup>	δ <sup>18</sup> O (‰VSMOW)	δ <sup>2</sup> H (‰VSMOW)	δ <sup>13</sup> C <sub>DIC</sub> (‰PDB)	a <sup>14</sup> C		<sup>3</sup> H	
														pMC	1σ	TU	1σ
<b>1a</b> (108899) <sup>a</sup>	29 <sup>b</sup>	282	60	0.18	35.1	4.8	2.9	2.2	0.23	0.14	-5.6	-32.7	-21.4	81	0.34	<i>bd</i> <sup>c</sup>	-
<b>1b</b> (108916)	14.5	197	38.6	0.12	29.3	3.4	4.1	1/9	0.24	0.09	-5.3	-30.4	-22.1	83.3	0.28	<i>bd</i>	-
<b>1c</b> (108917)	14.5	238	44	0.08	20.3	1.0	2.6	0.7	0.44	0.08	-5.3	-31.1	-21.5	77.8	0.29	<i>bd</i>	-
<b>2d</b> (108927)	14	430	86	0.07	69.1	16.3	9.9	7.4	0.5	0.36	-5.6	-32	-20	39.5	0.2	<i>bd</i>	-
<b>2e</b> (108928)	17	446	96	0.08	76.3	19.9	11	8.6	0.58	0.27	-5.5	-33.6	-19.8	40.9	0.21	<i>bd</i>	-
<b>3f</b> (108933)	11.2	491	121	0.1	84	8.6	5.3	9.1	0.52	0.16	-5.6	-34.1	-20.1	33.8	0.20	<i>bd</i>	-
<b>3g</b> (108934)	11.5	545	125	0.06	103.8	13.5	8.5	10.5	0.78	0.2	-5.8	-32.4	-20.4	29	0.16	<i>bd</i>	-
<b>3h</b> (108935)	11.5	144	27	0.04	19.9	1.7	2.7	0.7	0.12	0.07	-4.8	-31.2	-21.3	88.6	0.17	<i>bd</i>	-
<b>4i</b> (108940)	11.5	243	53	9.02	35.4	3.6	3.21	2.2	0.56	0.11	-5.8	-34	-22.3	64	0.24	<i>bd</i>	-
<b>4j</b> (108941)	11.5	414	89	0.03	80.3	7.1	3.9	11.5	0.64	0.03	-5.7	-34.3	-21.5	49	0.21	<i>bd</i>	-
<b>5k</b> (110737)	42	149	31	0.02	16.9	0.9	2.3	0.7	0.08	0.03	-5.1	-29.4	-22.4	100	0.3	1.24	0.06
<b>5l</b> (80732)	21	200	48	0.1	30	0.33	4.2	0.5	0	0.1	-4.5	-29.7	-24.2	101.5	0.17	1.02	0.03
<b>5m</b> (80735)	21	217	30	0.03	16.5	0.32	10.5	3.6	0	0.11	-4.2	-29.1	-25.3	100.7	0.17	1.47	0.04

1 **Table 2** – Radiocarbon ages of groundwater in the Gellibrand Catchment corrected for calcite  
 2 dissolution. Uncertainties are calculated varying q by  $\pm 0.1$  plus the analytical uncertainty of  $a^{14}\text{C}$   
 3 from *Table 1*

Sample	q	Radiocarbon Age (years)	Uncertainty
1a	0.93	1150	+ 630 / - 980
1b	0.96	1190	+ 360 / - 940
1c	0.93	1520	+ 590 / - 970
2d	0.86	6530	+ 940 / - 1050
2e	0.86	6170	+ 950 / - 1060
3f	0.87	7870	+ 950 / - 1050
3g	0.89	9260	+ 930 / - 1040
3h	0.93	380	+ 630 / - 380
4i	0.97	3440	+ 290 / - 930
4j	0.93	5310	+ 630 / - 980

## 29 **Figure Captions**

30

31 **Figure 1** – Geology, groundwater flow, and cross sectional view of the upper part of the Gellibrand  
32 River Catchment (the Gellibrand Valley). Potentiometric contours for the Eastern View Formation are  
33 created from groundwater data (Water Resources Data Warehouse, 2013) and are expressed in metres  
34 above Australian Height Datum (mAHD). Sampled groundwater bores are also shown. Letters refer to  
35 bores in Table 1.

36 **Figure 2** - (a) Groundwater elevations in bores display clear annual cycles (b) Groundwater head-  
37 gradients in the Gellibrand Valley are upwards implying a discharge zone (Victorian Water Resources  
38 Data Warehouse, 2013) (c) Flow in the Gellibrand River. Baseflow conditions during summer months  
39 transition into high flows in winter following winter rainfall. (Bureau of Meteorology, 2013)

40 **Figure 3** – Geochemical characteristics of groundwater in the Eastern View Formation; (a) mCl/Br v  
41 mCl (b) mNa/Cl v mCl (c) mCa v mHCO<sub>3</sub> (d) mSO<sub>4</sub> v mCa. Rainfall samples are also plotted where  
42 measured. Data is from Table 1 with repeat measurements over the sampling period included.

43 **Figure 4** – (a) <sup>2</sup>H vs <sup>18</sup>O values of the Gellibrand River and surrounding groundwater sampled over  
44 March 2011 – August 2013 and the weighted average for rainfall from Adelaide and Melbourne.  
45 MMWL = Melbourne Meteoric Water Line (Hughes and Crawford, 2012). GMWL = Global Meteoric  
46 Water Line (Clarke and Fritz, 1997). Groundwater with <sup>3</sup>H activities > 1 TU are also highlighted.  
47 Data is from Table 1 with repeat measurements over the sampling period included. (b) a<sup>14</sup>C vs <sup>18</sup>O of  
48 groundwater samples.

49 **Figure 5** - (a) Continuous electrical conductivity monitoring of near-river groundwater. **5** (b).  
50 Changes in river height over the study period. Groundwater EC and river level data from deployed  
51 Aqua troll 200 (In-Situ) Data Loggers.

52 **Figure 6** – Historical water table fluctuations 1988-2011 for bore 108927 (Victorian Water Resources  
53 Data Warehouse, 2013). The magnitude of annual recharge cycles are coherent with those recorded in  
54 data loggers over the study period (2011 to 2013)

55 **Figure 7** – Groundwater residence times within the Gellibrand Valley. Residence times up to 9260  
56 years are found in close proximity to the river. Modern local groundwaters with a<sup>14</sup>C > 100 pMC are  
57 situated back on the floodplain. Data from Tables 1 and 2.

58 **Figure 8** – Groundwater flow conceptualisation in the Gellibrand Valley. Though appreciable  
59 amounts of recharge are estimated from bore hydrographs and high river flows, the depth to which  
60 recharging waters infiltrate into the Eastern View Formation (downward leakage) is limited by strong  
61 upward head gradients, and a floodplain which consists of appreciable amounts of silt and clay.

62 **Figure 9** – <sup>14</sup>C age v Cl. <sup>14</sup>C ages are taken from the calcite corrected ages in *Table 1*

63

64

65

66